

# SELF-IMPROVING VISION-LANGUAGE-ACTION MODELS WITH DATA GENERATION VIA RESIDUAL RL

Anonymous authors

Paper under double-blind review

## ABSTRACT

Supervised fine-tuning (SFT) has become the de facto post-training strategy for large vision-language-action (VLA) models, but its reliance on costly human demonstrations limits scalability and generalization. We propose Probe, Learn, Distill (PLD), a three-stage plug-and-play framework that improves VLAs through residual reinforcement learning (RL) and distribution-aware data collection: train residual specialists to handle failure cases, collect deployment-aligned recovery data, and distill the resulting trajectories back into the generalist via SFT. We evaluate PLD across diverse settings: it achieves a near-saturated 99% task success rate on the LIBERO benchmark, delivers over 50% performance gains in SimplerEnv, and demonstrates a 100% success rate on real-world Franka arm and YAM arm dexterous manipulation tasks. We further provide ablations showing that residual policy probing and distribution-aware replay are key to collecting deployment-aligned data that improves VLAs’ capabilities on both seen and unseen tasks. Our results demonstrate that RL-generated, policy-aligned data can surpass teleoperation-only demonstrations, offering a scalable path toward self-improving VLA models.

## 1 INTRODUCTION

Supervised fine-tuning (SFT) has become the standard post-training paradigm for large language models (LLMs): after broad pre-training, models are adapted to downstream applications by training on curated instruction–response pairs, yielding many improvements in language following, safety, and generalization (Ouyang et al., 2022; Team, 2025). Inspired by these successes, the same recipe is now being applied to robot foundation models, particularly vision-language-action (VLA) policies, where large, heterogeneous robotics and vision-language datasets provide the base initialization, and

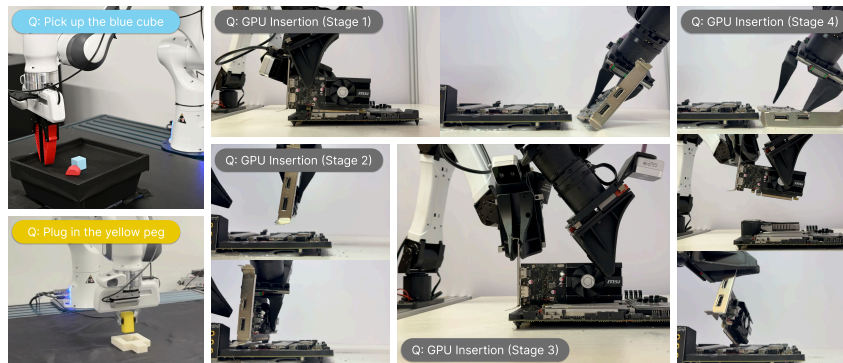


Figure 1: We demonstrate the performance of PLD on several real-world challenging manipulation tasks. The robot is successfully able to pick up diverse objects and conduct peg insertion for Franka arm. Besides, we also deploy PLD on YAM bi-manual settings, showing PLD policy continuously performs GPU insertion and unplugging cycle operating non-stop for 1 hour *without human resetting*. Check videos at [anonymous-pld.github.io](https://anonymous-pld.github.io)

SFT specializes models to specific tasks and embodiments (O’Neill et al., 2024; Team et al., 2024; Kim et al., 2024; 2025; Black et al., 2024; Bjorck et al., 2025). However, transferring this paradigm from language to robotics is a unique challenge. Collecting high-quality robot demonstrations is both costly and labor-intensive, making large-scale datasets much harder to obtain. Even when such data are available, they are often collected through teleoperation pipelines that are *decoupled* from the deployed VLA policy, leaving critical coverage gaps: human operators must manually anticipate and correct failure modes, but their demonstrations rarely reflect the actual distribution of states the policy will encounter at deployment. As a result, while SFT reliably improves performance on the tasks it is trained on, much less is understood about whether these gains transfer to new tasks and environments.

These challenges raise the following question: Can VLA models improve themselves using RL-curated data with minimal human effort? Specifically, can this self-curated training match or surpass fine-tuning on human-expert (oracle) teleoperation data, both in-distribution and out-of-distribution? Our central observation is that data collection should *not* be agnostic to the base policy: the data-collecting policy and the generalist must *interact*, so that exploration leverages the generalist’s prior knowledge and collected data remain aligned with its trajectory distribution.

Motivated by these challenges, we introduce **PLD**, a three-stage post-training pipeline. **Stage 1: Online specialist acquisition.** We freeze the VLA backbone and train several lightweight *residual* actors for multiple tasks via sample-efficient off-policy RL, enabling them to “take over” the base policy at arbitrary states and achieve above 99% task success. **Stage 2: Automatic data collection.** We propose a hybrid rollout scheme that biases residual takeovers toward states frequently visited by the base model, mitigating distribution shift while capturing recovery behaviors. **Stage 3: Supervised fine-tuning.** The collected data for multiple tasks are distilled back into the base model through SFT, a process agnostic to VLA architectures, supporting both flow-matching and autoregressive action heads (Black et al., 2024; Kim et al., 2024). An overview of our pipeline can be found in Figure 4. With **PLD**, we can efficiently acquire task-specific RL experts through VLA-guided exploration. Consequently, the VLA further improves using the **PLD** data, achieving performance above 99% on the LIBERO benchmark.

This paper makes the following contributions: 1) Autonomous post-training recipe. We propose a post-training pipeline that enables VLA models to improve autonomously without relying on additional oracle demonstrations. Our method achieves near-saturated 99% success rates on the LIBERO benchmark, and delivers over 50% performance gains in SimplerEnv, underscoring both its effectiveness on seen tasks and its ability to generalize to unseen ones. 2) Systematic study of RL-generated data. We analyze the key components of automatic data collection most beneficial for SFT, and conduct extensive experiments in simulation and on real robot hardware to examine how *RL-generated data* influences generalization to unseen tasks. 3) Comprehensive empirical validation. We provide large-scale ablations of our design choices. Besides, we showcase >99% success rate on Franka Arm and YAM arm dexterous manipulation tasks. Achieving continuous GPU insertion and unplugging operating for 1 hour without human intervention, offering potential for data-efficient post-training of robot foundation models.

## 2 METHODS

We study the synergy between the data produced by our method when a modest *generalist* VLA serves as the prior policy. The premise is that, if we exploit the base policy’s prior correctly, it can both *solve hard tasks quickly* and *explore efficiently*. While recent work explores direct RL fine-tuning of expressive policy class (Mark et al., 2024; Dong et al., 2025b), such a formulation can be resource-intensive even for single-task tuning: e.g., OpenVLA-OFT requires per-GPU memory up to  $\sim 62.5$  GB for LIBERO training at batch size 8 (Kim et al., 2025). Meanwhile, it remains unclear whether these approaches scale gracefully to multi-task fine-tuning under heterogeneous setups. We therefore opt for a *decoupled* pipeline. We freeze the base policy  $\pi_b$  and learn a lightweight residual action policy  $\pi_\delta$  with sample-efficient off-policy RL (Gaussian policy parameterization). We then *collect expert data* by letting the residual “take over” after specified steps of “base policy probing”. Finally, we *distill* these skills back into the base model via SFT and deploy the generalist on diverse manipulation tasks. We provide the overview of **PLD** in Figure 4. Due to the page limit, we postpone the detailed analysis to the appendix B.

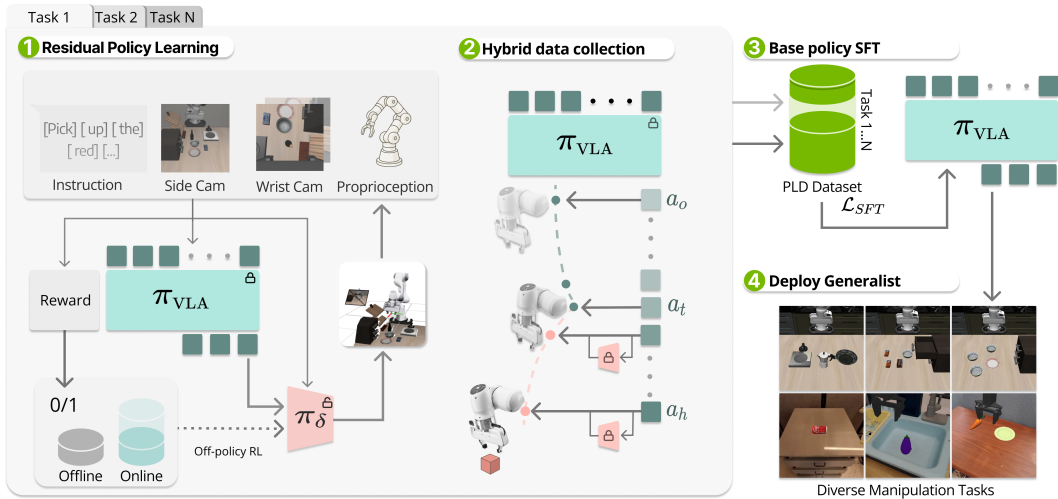


Figure 2: **An overview of PLD.** Our pipeline consists of three stages: 1) learning specialist residual policy for each task via online off-policy RL, with efficient exploration guided by a frozen VLA generalist; 2) Automatic generation of hybrid trajectories by having the VLA rollout for the first  $t$  steps and let the specialist takeover to generate recover data; 3) Supervised fine-tuning using collected multi-task PLD data; 4) Deploy the fine-tuned generalist to diverse manipulation tasks in zero-shot.

### 3 EXPERIMENTS

In this section, we systematically evaluate the effectiveness of PLD. We first demonstrate the efficiency of PLD-RL in solving sparse-reward manipulation tasks, which serves as the cornerstone of our pipeline. Then we focus on study 1) How does the probing mechanism of PLD benefit VLA SFT; 2) How does PLD data compare with other sources of demonstrations. Finally, we investigate the key factors of our pipeline and how they contribute to improving the performance of VLA.

We consider simulation as a proxy to real-world performance, and evaluate methods across two widely adopted simulation benchmarks, including LIBERO (Liu et al., 2023), SimplerEnv (Li et al., 2024). LIBERO is a lifelong learning benchmark focused on language-guided manipulation tasks. It comprises 130 tasks grouped into four suites that stress object distribution, spatial arrangement, task goals, and their mixture. SimplerEnv is a robotics manipulation benchmark that aims for high sim-to-real correlation.

In the following sections, we will be mainly analyzing different data sources: PLD data  $\mathcal{D}^{\text{PLD}}$ , Human data  $\mathcal{D}^{\text{Human}}$ , RL expert data (RL expert rollout w/o base policy probing)  $\mathcal{D}^{\text{RL}}$ , and base-policy rollout data (Selective successful rollouts, also referred to as "self-bootstrap data")  $\mathcal{D}^{\text{Base Policy}}$ . Unless stated otherwise, all methods use identical data volume, training budgets, augmentation, and hyperparameters across architectures; the default base policy we used is  $\pi_0$  (Black et al., 2024).

#### 3.1 EFFECTIVENESS AND EFFICIENCY OF LEARNING RL SPECIALIST

In this section, we seek answers to the following questions: Does PLD benefit from both policy guidance and hybrid online learning? We compare state-of-the-art methods that leverage policy priors and data priors: WSRL (Zhou et al., 2024b) (offline initialization only); RLPD (Ball et al., 2023) (No base policy guidance). For the pre-training stage, we collect a dataset of 50 trajectories per task, containing only the successful trials of the same base policy ( $\pi_0$ ), and using Cal-QL (Nakamoto et al., 2024) as the default pre-training algorithm. Subsequently, we retain these data for methods with online hybrid data replay. We plot the training curve of 250k steps of online interaction, showing mean rollout performance and 95% CIs (confidence level) across 3 seeds in Figure 3.

PLD outperforms baseline methods by a large margin across 8 tasks on LIBERO-90, indicating that PLD effectively exploits the VLA policy prior and yields pronounced sample efficiency at low in-

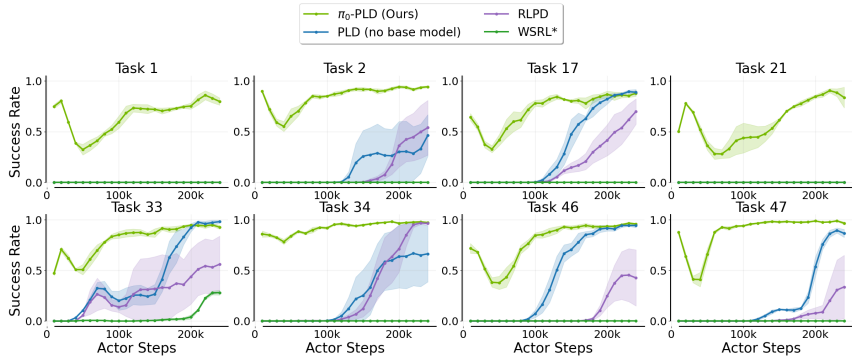


Figure 3: **Benchmarking Sample-Efficient RL Performance.** We compare **PLD** with RL baseline algorithms that either leverage policy prior or data prior. We report mean rollout performance (Average return calculated within a sliding window of 100 episodes) and 95% CIs for 3 seeds across 8 manipulation tasks selected from LIBERO-90.

teraction budgets. In terms of asymptotic performance, **PLD** can achieve *over 95% performance* on every task that we report to fine-tune performance (over **120** manipulation tasks). Notably, we observe an initial performance drop for **PLD**. This phenomenon implies the initial phase of exploration, where the residual policy starts to diverge from the base policy and visits potentially suboptimal states. Ablation study on **PLD**-RL’s design choice can be found in the Section [F.2](#).

### 3.2 GENERALIZATION

**Generalization to Unseen tasks** To study the synergetic effect of **PLD** data, we examine whether **PLD** data improves *zero-shot* performance on unseen tasks in the LIBERO benchmark (Liu et al., 2023). Concretely, we fine-tune  $\pi_0$  via SFT using data drawn from the disjoint *coverage subsets* of LIBERO-90 in proportions  $\{0.1, 0.3, 0.6, 0.8, 1.0\}$ ; for each coverage level, we randomly sample tasks to form a new subset in distribution and then evaluate all tasks in the suite. We sampled 4 subsets for each coverage level to provide a more unified result. We consider three different data sources: (i) Ours  $\mathcal{D}^{PLD}$ , (ii) human expert data  $\mathcal{D}^{Human}$ , and (iii) *self-bootstrapping* data  $\mathcal{D}^{\pi_0}$  rollout (SFT on this variant corresponds to 0-1 REINFORCE (Shenfeld et al., 2025)). We visualize the result in Figure 5. Across coverage levels,  $\pi_0$  fine-tuned on  $\mathcal{D}^{PLD}$  attains the strongest in-distribution performance and maintains robust zero-shot transfer to unseen tasks; human data-only SFT achieves approximately a similar level of zero-shot generalization at the same training budget but lags on in-distribution tasks;  $\pi_0$  self-bootstrapping rollout data underperforms in-distribution and fails to generalize to out-of-distribution tasks.

**Generalization to Out-of-domain** We study *few-shot generalization* for tasks with different goals, layouts, and backgrounds. We first collect **PLD** data of varying scales set on *source* tasks (LIBERO-Goal) and evaluate the fine-tuning performance on *target* tasks (LIBERO-90). Specifically, the VLA is fine-tuned on **PLD** data of source tasks *plus* a small number of oracle demos of target tasks. To analyze transfer by skill family, we select tasks from LIBERO-goal and LIBERO-90 that have high semantic correlation to form a set of source/target tasks. We scaled the size of  $|\mathcal{D}^{PLD}|$  from 50 to 500 trajectories and compared against  $\mathcal{D}^{RL}$  and  $\mathcal{D}^{BS}$  under the same data and training budget. As shown in Figure 8, we observe monotonic improvements in SFT performance as the data scales from 50 to 500 trajectories.

### 3.3 REAL-WORLD EVALUATION

We evaluate our approach on a 7-DoF Franka Emika Panda arm in the real world, considering two sets of canonical manipulation tasks: *pick-and-place* and *peg insertion*, illustrated in Figure 19. Unlike prior works (Luo et al., 2025; Zhou et al., 2024b), we do not restrict task randomization, making real-world reinforcement learning particularly challenging. A more detailed experimental setup is provided in Section [H](#).

## REFERENCES

- 216  
217  
218 Lars Ankile, Anthony Simeonov, Idan Shenfeld, Marcel Torne, and Pulkit Agrawal. From imitation  
219 to refinement-residual rl for precise assembly. In *2025 IEEE International Conference on Robotics  
220 and Automation (ICRA)*, pp. 01–08. IEEE, 2025.
- 221 Jimmy Lei Ba, Jamie Ryan Kiros, and Geoffrey E Hinton. Layer normalization. *arXiv preprint  
222 arXiv:1607.06450*, 2016.
- 223 Philip J Ball, Laura Smith, Ilya Kostrikov, and Sergey Levine. Efficient online reinforcement learn-  
224 ing with offline data. In *International Conference on Machine Learning*, pp. 1577–1594. PMLR,  
225 2023.
- 226 Johan Bjorck, Fernando Castañeda, Nikita Cherniadev, Xingye Da, Runyu Ding, Linxi Fan,  
227 Yu Fang, Dieter Fox, Fengyuan Hu, Spencer Huang, et al. Gr00t n1: An open foundation model  
228 for generalist humanoid robots. *arXiv preprint arXiv:2503.14734*, 2025.
- 230 Kevin Black, Noah Brown, Danny Driess, Adnan Esmail, Michael Equi, Chelsea Finn, Niccolo  
231 Fusai, Lachy Groom, Karol Hausman, Brian Ichter, et al.  $\pi_0$ : A vision-language-action flow  
232 model for general robot control. *arXiv preprint arXiv:2410.24164*, 2024.
- 233 James Bradbury, Roy Frostig, Peter Hawkins, Matthew James Johnson, Chris Leary, Dougal  
234 Maclaurin, George Necula, Adam Paszke, Jake VanderPlas, Skye Wanderman-Milne, and Qiao  
235 Zhang. JAX: composable transformations of Python+NumPy programs, 2018. URL [http://  
236 github.com/google/jax](http://github.com/google/jax).
- 237 Anthony Brohan, Noah Brown, Justice Carbajal, Yevgen Chebotar, Xi Chen, Krzysztof Choro-  
238 manski, Tianli Ding, Danny Driess, Avinava Dubey, Chelsea Finn, Pete Florence, Chuyuan Fu,  
239 Montse Gonzalez Arenas, Keerthana Gopalakrishnan, Kehang Han, Karol Hausman, Alexander  
240 Herzog, Jasmine Hsu, Brian Ichter, Alex Irpan, Nikhil Joshi, Ryan Julian, Dmitry Kalashnikov,  
241 Yuheng Kuang, Isabel Leal, Lisa Lee, Tsang-Wei Edward Lee, Sergey Levine, Yao Lu, Hen-  
242 ryk Michalewski, Igor Mordatch, Karl Pertsch, Kanishka Rao, Krista Reymann, Michael Ryoo,  
243 Grecia Salazar, Pannag Sanketi, Pierre Sermanet, Jaspiar Singh, Anikait Singh, Radu Soricut,  
244 Huang Tran, Vincent Vanhoucke, Quan Vuong, Ayzaan Wahid, Stefan Welker, Paul Wohlhart,  
245 Jialin Wu, Fei Xia, Ted Xiao, Peng Xu, Sichun Xu, Tianhe Yu, and Brianna Zitkovich. Rt-  
246 2: Vision-language-action models transfer web knowledge to robotic control, 2023a. URL  
247 <https://arxiv.org/abs/2307.15818>.
- 248 Anthony Brohan, Noah Brown, Justice Carbajal, Yevgen Chebotar, Joseph Dabis, Chelsea Finn,  
249 Keerthana Gopalakrishnan, Karol Hausman, Alex Herzog, Jasmine Hsu, Julian Ibarz, Brian  
250 Ichter, Alex Irpan, Tomas Jackson, Sally Jesmonth, Nikhil J Joshi, Ryan Julian, Dmitry Kalash-  
251 nikov, Yuheng Kuang, Isabel Leal, Kuang-Huei Lee, Sergey Levine, Yao Lu, Utsav Malla, Deek-  
252 sha Manjunath, Igor Mordatch, Ofir Nachum, Carolina Parada, Jodilyn Peralta, Emily Perez,  
253 Karl Pertsch, Jornell Quiambao, Kanishka Rao, Michael Ryoo, Grecia Salazar, Pannag Sanketi,  
254 Kevin Sayed, Jaspiar Singh, Sumedh Sontakke, Austin Stone, Clayton Tan, Huang Tran, Vin-  
255 cent Vanhoucke, Steve Vega, Quan Vuong, Fei Xia, Ted Xiao, Peng Xu, Sichun Xu, Tianhe Yu,  
256 and Brianna Zitkovich. Rt-1: Robotics transformer for real-world control at scale, 2023b. URL  
257 <https://arxiv.org/abs/2212.06817>.
- 258 Tom Brown, Benjamin Mann, Nick Ryder, Melanie Subbiah, Jared D Kaplan, Prafulla Dhari-  
259 wal, Arvind Neelakantan, Pranav Shyam, Girish Sastry, Amanda Askell, Sandhini Agar-  
260 wal, Ariel Herbert-Voss, Gretchen Krueger, Tom Henighan, Rewon Child, Aditya Ramesh,  
261 Daniel Ziegler, Jeffrey Wu, Clemens Winter, Chris Hesse, Mark Chen, Eric Sigler, Mateusz  
262 Litwin, Scott Gray, Benjamin Chess, Jack Clark, Christopher Berner, Sam McCandlish, Alec  
263 Radford, Ilya Sutskever, and Dario Amodei. Language models are few-shot learners. In  
264 H. Larochelle, M. Ranzato, R. Hadsell, M.F. Balcan, and H. Lin (eds.), *Advances in Neu-  
265 ral Information Processing Systems*, volume 33, pp. 1877–1901. Curran Associates, Inc.,  
266 2020. URL [https://proceedings.neurips.cc/paper\\_files/paper/2020/  
267 file/1457c0d6bfc4967418bfb8ac142f64a-Paper.pdf](https://proceedings.neurips.cc/paper_files/paper/2020/file/1457c0d6bfc4967418bfb8ac142f64a-Paper.pdf).
- 268 Xi Chen, Xiao Wang, Soravit Changpinyo, Piotr Padlewski, Daniel Salz, Sebastian Goodman, Adam  
269 Grycner, Basil Mustafa, Lucas Beyer, et al. Pali: A jointly-scaled multilingual language-image  
model. *arXiv preprint arXiv:2209.06794*, 2022.

- 270 Xinlei Chen, Hao Fang, Tsung-Yi Lin, Ramakrishna Vedantam, Saurabh Gupta, Piotr Dollar, and  
271 C. Lawrence Zitnick. Microsoft coco captions: Data collection and evaluation server, 2015. URL  
272 <https://arxiv.org/abs/1504.00325>.
- 273
- 274 Yuhui Chen, Shuai Tian, Shugao Liu, Yingting Zhou, Haoran Li, and Dongbin Zhao. Con-  
275 firt: A reinforced fine-tuning method for vla models via consistency policy. *arXiv preprint*  
276 *arXiv:2502.05450*, 2025.
- 277 Cheng Chi, Zhenjia Xu, Siyuan Feng, Eric Cousineau, Yilun Du, Benjamin Burchfiel, Russ Tedrake,  
278 and Shuran Song. Diffusion policy: Visuomotor policy learning via action diffusion, 2024. URL  
279 <https://arxiv.org/abs/2303.04137>.
- 280
- 281 Perry Dong, Alec M Lessing, Annie S Chen, and Chelsea Finn. Reinforcement learning via implicit  
282 imitation guidance. *arXiv preprint arXiv:2506.07505*, 2025a.
- 283
- 284 Perry Dong, Qiyang Li, Dorsa Sadigh, and Chelsea Finn. Expo: Stable reinforcement learning with  
285 expressive policies. *arXiv preprint arXiv:2507.07986*, 2025b.
- 286
- 287 Justin Fu, Aviral Kumar, Ofir Nachum, George Tucker, and Sergey Levine. D4rl: Datasets for deep  
288 data-driven reinforcement learning. *arXiv preprint arXiv:2004.07219*, 2020.
- 289
- 290 Scott Fujimoto, Herke Hoof, and David Meger. Addressing function approximation error in actor-  
291 critic methods. In *International conference on machine learning*, pp. 1587–1596. PMLR, 2018.
- 292
- 293 Yash Goyal, Tejas Khot, Douglas Summers-Stay, Dhruv Batra, and Devi Parikh. Making the v in vqa  
294 matter: Elevating the role of image understanding in visual question answering. In *Proceedings*  
295 *of the IEEE conference on computer vision and pattern recognition*, pp. 6904–6913, 2017.
- 296
- 297 Siddhant Haldar, Jyothish Pari, Anant Rai, and Lerrel Pinto. Teach a robot to fish: Versatile imitation  
298 from one minute of demonstrations. *arXiv preprint arXiv:2303.01497*, 2023.
- 299
- 300 Jonathan Ho, Ajay Jain, and Pieter Abbeel. Denoising diffusion probabilistic models, 2020. URL  
301 <https://arxiv.org/abs/2006.11239>.
- 302
- 303 Edward J. Hu, Yelong Shen, Phillip Wallis, Zeyuan Allen-Zhu, Yuanzhi Li, Shean Wang, Lu Wang,  
304 and Weizhu Chen. Lora: Low-rank adaptation of large language models, 2021. URL <https://arxiv.org/abs/2106.09685>.
- 305
- 306 I2RT-Robotics. Yam – 6-dof robotic arm. [https://i2rt.com/products/](https://i2rt.com/products/yam-manipulator)  
307 [yam-manipulator](https://i2rt.com/products/yam-manipulator), 2025.
- 308
- 309 Physical Intelligence, Kevin Black, Noah Brown, James Darpinian, Karan Dhabalia, Danny Driess,  
310 Adnan Esmail, Michael Equi, Chelsea Finn, Niccolo Fusai, et al.  $\pi_{0.5}$ : a vision-language-  
311 action model with open-world generalization. *arXiv preprint arXiv:2504.16054*, 2025.
- 312
- 313 Tobias Jülg, Wolfram Burgard, and Florian Walter. Refined policy distillation: From vla generalists  
314 to rl experts. *arXiv preprint arXiv:2503.05833*, 2025.
- 315
- 316 Michael Kelly, Chelsea Sidrane, Katherine Driggs-Campbell, and Mykel J Kochenderfer. Hg-  
317 dagger: Interactive imitation learning with human experts. In *2019 International Conference*  
318 *on Robotics and Automation (ICRA)*, pp. 8077–8083. IEEE, 2019.
- 319
- 320 Alexander Khazatsky, Karl Pertsch, Suraj Nair, Ashwin Balakrishna, Sudeep Dasari, Siddharth  
321 Karamcheti, Soroush Nasiriany, Mohan Kumar Srirama, Lawrence Yunliang Chen, Kirsty Ellis,  
322 Peter David Fagan, Joey Hejna, Masha Itkina, Marion Lepert, Yecheng Jason Ma, Patrick Tree  
323 Miller, Jimmy Wu, Suneel Belkhale, Shivin Dass, Huy Ha, Arhan Jain, Abraham Lee, Young-  
woon Lee, Marius Memmel, Sungjae Park, Ilija Radosavovic, Kaiyuan Wang, Albert Zhan, Kevin  
Black, Cheng Chi, Kyle Beltran Hatch, Shan Lin, Jingpei Lu, Jean Mercat, Abdul Rehman,  
Pannag R Sanketi, Archit Sharma, Cody Simpson, Quan Vuong, Homer Rich Walke, Blake  
Wulfe, Ted Xiao, Jonathan Heewon Yang, Arefeh Yavary, Tony Z. Zhao, Christopher Agia, Ro-  
han Baijal, Mateo Guaman Castro, Daphne Chen, Qiuyu Chen, Trinity Chung, Jaimyn Drake,  
Ethan Paul Foster, Jensen Gao, Vitor Guizilini, David Antonio Herrera, Minh Heo, Kyle  
Hsu, Jiaheng Hu, Muhammad Zubair Irshad, Donovan Jackson, Charlotte Le, Yunshuang Li,

- 324 Kevin Lin, Roy Lin, Zehan Ma, Abhiram Maddukuri, Suvir Mirchandani, Daniel Morton, Tony  
325 Nguyen, Abigail O’Neill, Rosario Scalise, Derick Seale, Victor Son, Stephen Tian, Emi Tran, An-  
326 drew E. Wang, Yilin Wu, Annie Xie, Jingyun Yang, Patrick Yin, Yunchu Zhang, Osbert Bastani,  
327 Glen Berseth, Jeannette Bohg, Ken Goldberg, Abhinav Gupta, Abhishek Gupta, Dinesh Jayara-  
328 man, Joseph J Lim, Jitendra Malik, Roberto Martín-Martín, Subramanian Ramamoorthy, Dorsa  
329 Sadigh, Shuran Song, Jiajun Wu, Michael C. Yip, Yuke Zhu, Thomas Kollar, Sergey Levine,  
330 and Chelsea Finn. Droid: A large-scale in-the-wild robot manipulation dataset, 2025. URL  
331 <https://arxiv.org/abs/2403.12945>.
- 332 Moo Jin Kim, Karl Pertsch, Siddharth Karamcheti, Ted Xiao, Ashwin Balakrishna, Suraj Nair,  
333 Rafael Rafailov, Ethan Foster, Grace Lam, Pannag Sanketi, et al. Openvla: An open-source  
334 vision-language-action model. *arXiv preprint arXiv:2406.09246*, 2024.
- 335 Moo Jin Kim, Chelsea Finn, and Percy Liang. Fine-tuning vision-language-action models: Opti-  
336 mizing speed and success. *arXiv preprint arXiv:2502.19645*, 2025.
- 337 Ilya Kostrikov, Ashvin Nair, and Sergey Levine. Offline reinforcement learning with implicit q-  
338 learning. *arXiv preprint arXiv:2110.06169*, 2021.
- 339 Aviral Kumar, Aurick Zhou, George Tucker, and Sergey Levine. Conservative q-learning for offline  
340 reinforcement learning. *Advances in neural information processing systems*, 33:1179–1191, 2020.
- 341 Sergey Levine, Aviral Kumar, George Tucker, and Justin Fu. Offline reinforcement learning: Tuto-  
342 rial, review, and perspectives on open problems. *arXiv preprint arXiv:2005.01643*, 2020.
- 343 Qiyang Li, Zhiyuan Zhou, and Sergey Levine. Reinforcement learning with action chunking. *arXiv*  
344 *preprint arXiv:2507.07969*, 2025.
- 345 Xuanlin Li, Kyle Hsu, Jiayuan Gu, Karl Pertsch, Oier Mees, Homer Rich Walke, Chuyuan Fu,  
346 Ishikaa Lunawat, Isabel Sieh, Sean Kirmani, et al. Evaluating real-world robot manipulation  
347 policies in simulation. *arXiv preprint arXiv:2405.05941*, 2024.
- 348 Timothy P Lillicrap, Jonathan J Hunt, Alexander Pritzel, Nicolas Heess, Tom Erez, Yuval Tassa,  
349 David Silver, and Daan Wierstra. Continuous control with deep reinforcement learning. *arXiv*  
350 *preprint arXiv:1509.02971*, 2015.
- 351 Bo Liu, Yifeng Zhu, Chongkai Gao, Yihao Feng, Qiang Liu, Yuke Zhu, and Peter Stone. Libero:  
352 Benchmarking knowledge transfer for lifelong robot learning. *Advances in Neural Information*  
353 *Processing Systems*, 36:44776–44791, 2023.
- 354 Guanxing Lu, Wenkai Guo, Chubin Zhang, Yuheng Zhou, Haonan Jiang, Zifeng Gao, Yansong  
355 Tang, and Ziwei Wang. V1a-rl: Towards masterful and general robotic manipulation with scalable  
356 reinforcement learning. *arXiv preprint arXiv:2505.18719*, 2025.
- 357 Jianlan Luo, Zheyuan Hu, Charles Xu, You Liang Tan, Jacob Berg, Archit Sharma, Stefan Schaal,  
358 Chelsea Finn, Abhishek Gupta, and Sergey Levine. Serl: A software suite for sample-efficient  
359 robotic reinforcement learning. In *2024 IEEE International Conference on Robotics and Automa-*  
360 *tion (ICRA)*, pp. 16961–16969. IEEE, 2024.
- 361 Jianlan Luo, Charles Xu, Jeffrey Wu, and Sergey Levine. Precise and dexterous robotic manipulation  
362 via human-in-the-loop reinforcement learning. *Science Robotics*, 10(105):eads5033, 2025.
- 363 Max Sobol Mark, Tian Gao, Georgia Gabriela Sampaio, Mohan Kumar Srirama, Archit Sharma,  
364 Chelsea Finn, and Aviral Kumar. Policy agnostic rl: Offline rl and online rl fine-tuning of any  
365 class and backbone. *arXiv preprint arXiv:2412.06685*, 2024.
- 366 Ashvin Nair, Abhishek Gupta, Murtaza Dalal, and Sergey Levine. Awac: Accelerating online rein-  
367 forcement learning with offline datasets. *arXiv preprint arXiv:2006.09359*, 2020.
- 368 Mitsuhiko Nakamoto, Simon Zhai, Anikait Singh, Max Sobol Mark, Yi Ma, Chelsea Finn, Aviral  
369 Kumar, and Sergey Levine. Cal-ql: Calibrated offline rl pre-training for efficient online fine-  
370 tuning. *Advances in Neural Information Processing Systems*, 36, 2024.
- 371
- 372
- 373
- 374
- 375
- 376
- 377

- 378 Long Ouyang, Jeff Wu, Xu Jiang, Diogo Almeida, Carroll L. Wainwright, Pamela Mishkin, Chong  
379 Zhang, Sandhini Agarwal, Katarina Slama, Alex Ray, John Schulman, Jacob Hilton, Fraser Kel-  
380 ton, Luke Miller, Maddie Simens, Amanda Askell, Peter Welinder, Paul Christiano, Jan Leike,  
381 and Ryan Lowe. Training language models to follow instructions with human feedback, 2022.  
382 URL <https://arxiv.org/abs/2203.02155>.
- 383  
384 Abby O’Neill, Abdul Rehman, Abhiram Maddukuri, Abhishek Gupta, Abhishek Padalkar, Abraham  
385 Lee, Acorn Pooley, Agrim Gupta, Ajay Mandlekar, Ajinkya Jain, et al. Open x-embodiment:  
386 Robotic learning datasets and rt-x models: Open x-embodiment collaboration 0. In *2024 IEEE*  
387 *International Conference on Robotics and Automation (ICRA)*, pp. 6892–6903. IEEE, 2024.
- 388 Karl Pertsch, Kyle Stachowicz, Brian Ichter, Danny Driess, Suraj Nair, Quan Vuong, Oier Mees,  
389 Chelsea Finn, and Sergey Levine. Fast: Efficient action tokenization for vision-language-action  
390 models. *arXiv preprint arXiv:2501.09747*, 2025.
- 391  
392 John Schulman, Filip Wolski, Prafulla Dhariwal, Alec Radford, and Oleg Klimov. Proximal policy  
393 optimization algorithms. *arXiv preprint arXiv:1707.06347*, 2017.
- 394  
395 Archit Sharma, Ahmed M Ahmed, Rehaan Ahmad, and Chelsea Finn. Self-improving robots: End-  
396 to-end autonomous visuomotor reinforcement learning. *arXiv preprint arXiv:2303.01488*, 2023.
- 397  
398 Idan Shenfeld, Jyothish Pari, and Pulkit Agrawal. RL’s razor: Why online reinforcement learning  
399 forgets less. *arXiv preprint arXiv:2509.04259*, 2025.
- 400  
401 Yuda Song, Yifei Zhou, Ayush Sekhari, J Andrew Bagnell, Akshay Krishnamurthy, and Wen  
402 Sun. Hybrid rl: Using both offline and online data can make rl efficient. *arXiv preprint*  
403 *arXiv:2210.06718*, 2022.
- 404  
405 Yuda Song, J Andrew Bagnell, and Aarti Singh. Hybrid reinforcement learning from offline obser-  
406 vation alone. *arXiv preprint arXiv:2406.07253*, 2024.
- 407  
408 Richard S Sutton and Andrew G Barto. *Reinforcement learning: An introduction*. MIT press, 2018.
- 409  
410 Shuhan Tan, Kairan Dou, Yue Zhao, and Philipp Krähenbühl. Interactive post-training for vision-  
411 language-action models. *arXiv preprint arXiv:2505.17016*, 2025.
- 412  
413 Gemini Team. Gemini: A family of highly capable multimodal models, 2025. URL <https://arxiv.org/abs/2312.11805>.
- 414  
415 Octo Model Team, Dibya Ghosh, Homer Walke, Karl Pertsch, Kevin Black, Oier Mees, Sudeep  
416 Dasari, Joey Hejna, Tobias Kreiman, Charles Xu, et al. Octo: An open-source generalist robot  
417 policy. *arXiv preprint arXiv:2405.12213*, 2024.
- 418  
419 Hugo Touvron, Louis Martin, Kevin Stone, Peter Albert, Amjad Almahairi, Yasmine Babaei, Niko-  
420 lay Bashlykov, Soumya Batra, Prajjwal Bhargava, Shruti Bhosale, Dan Bikel, Lukas Blecher,  
421 Cristian Canton Ferrer, Moya Chen, Guillem Cucurull, David Esiobu, Jude Fernandes, Jeremy  
422 Fu, Wenyin Fu, Brian Fuller, Cynthia Gao, Vedanuj Goswami, Naman Goyal, Anthony Hartshorn,  
423 Saghar Hosseini, Rui Hou, Hakan Inan, Marcin Kardas, Viktor Kerkez, Madian Khabsa, Isabel  
424 Kloumann, Artem Korenev, Punit Singh Koura, Marie-Anne Lachaux, Thibaut Lavril, Jenya Lee,  
425 Diana Liskovich, Yinghai Lu, Yuning Mao, Xavier Martinet, Todor Mihaylov, Pushkar Mishra,  
426 Igor Molybog, Yixin Nie, Andrew Poulton, Jeremy Reizenstein, Rashi Rungta, Kalyan Saladi,  
427 Alan Schelten, Ruan Silva, Eric Michael Smith, Ranjan Subramanian, Xiaoqing Ellen Tan, Binh  
428 Tang, Ross Taylor, Adina Williams, Jian Xiang Kuan, Puxin Xu, Zheng Yan, Iliyan Zarov, Yuchen  
429 Zhang, Angela Fan, Melanie Kambadur, Sharan Narang, Aurelien Rodriguez, Robert Stojnic,  
430 Sergey Edunov, and Thomas Scialom. Llama 2: Open foundation and fine-tuned chat models,  
431 2023. URL <https://arxiv.org/abs/2307.09288>.
- 430 Ikechukwu Uchendu, Ted Xiao, Yao Lu, Banghua Zhu, Mengyuan Yan, Joséphine Simon, Matthew  
431 Bennis, Chuyuan Fu, Cong Ma, Jiantao Jiao, et al. Jump-start reinforcement learning. In *Inter-  
national Conference on Machine Learning*, pp. 34556–34583. PMLR, 2023.

432 Mel Vecerik, Todd Hester, Jonathan Scholz, Fumin Wang, Olivier Pietquin, Bilal Piot, Nico-  
433 las Heess, Thomas Rothörl, Thomas Lampe, and Martin Riedmiller. Leveraging demonstra-  
434 tions for deep reinforcement learning on robotics problems with sparse rewards. *arXiv preprint*  
435 *arXiv:1707.08817*, 2017.

436 Homer Rich Walke, Jonathan Heewon Yang, Albert Yu, Aviral Kumar, Jędrzej Orbik, Avi Singh, and  
437 Sergey Levine. Don’t start from scratch: Leveraging prior data to automate robotic reinforcement  
438 learning. In *Conference on Robot Learning*, pp. 1652–1662. PMLR, 2023.

439  
440 Haoru Xue, Xiaoyu Huang, Dantong Niu, Qiayuan Liao, Thomas Kragerud, Jan Tommy Grav-  
441 dahl, Xue Bin Peng, Guanya Shi, Trevor Darrell, Koushil Sreenath, and Shankar Sastry. Le-  
442 verb: Humanoid whole-body control with latent vision-language instruction, 2025. URL <https://arxiv.org/abs/2506.13751>.

443  
444 Weirui Ye, Yunsheng Zhang, Haoyang Weng, Xianfan Gu, Shengjie Wang, Tong Zhang, Mengchen  
445 Wang, Pieter Abbeel, and Yang Gao. Reinforcement learning with foundation priors: Let the  
446 embodied agent efficiently learn on its own. *arXiv preprint arXiv:2310.02635*, 2023.

447  
448 Kelin Yu, Yunhai Han, Qixian Wang, Vaibhav Saxena, Danfei Xu, and Ye Zhao. Mimictouch: Lever-  
449 aging multi-modal human tactile demonstrations for contact-rich manipulation. *arXiv preprint*  
450 *arXiv:2310.16917*, 2023.

451  
452 Zhiyuan Zhou, Pranav Atreya, Abraham Lee, Homer Walke, Oier Mees, and Sergey Levine. Au-  
453 tonomous improvement of instruction following skills via foundation models. *arXiv preprint*  
454 *arXiv:2407.20635*, 2024a.

455  
456 Zhiyuan Zhou, Andy Peng, Qiyang Li, Sergey Levine, and Aviral Kumar. Efficient online reinforce-  
457 ment learning fine-tuning need not retain offline data. *arXiv preprint arXiv:2412.07762*, 2024b.

458  
459  
460  
461  
462  
463  
464  
465  
466  
467  
468  
469  
470  
471  
472  
473  
474  
475  
476  
477  
478  
479  
480  
481  
482  
483  
484  
485

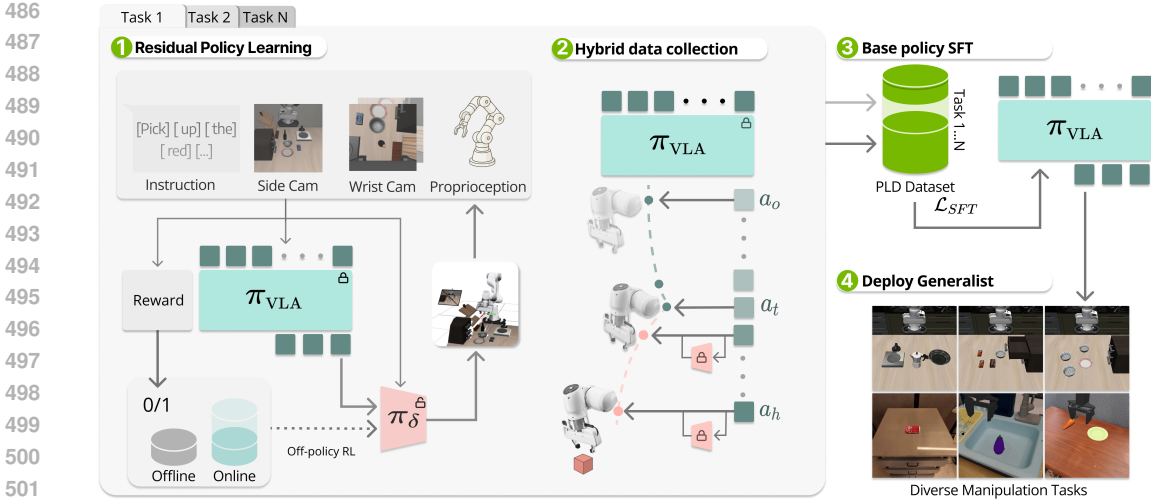


Figure 4: **An overview of PLD.** Our pipeline consists of three stages: 1) learning specialist residual policy for each task via online off-policy RL, with efficient exploration guided by a frozen VLA generalist; 2) Automatic generation of hybrid trajectories by having the VLA rollout for the first  $t$  steps and let the specialist takeover to generate recover data; 3) Supervised fine-tuning using collected multi-task PLD data; 4) Deploy the fine-tuned generalist to diverse manipulation tasks in zero-shot.

## A LARGE LANGUAGE MODEL USAGE STATEMENT

We used the large language model ChatGPT *only* for writing assistance, including grammar correction, wording improvements, and minor stylistic edits on draft text. The model was **not** used for research ideation, data collection, dataset labeling, code generation, experiment design, or analysis. All technical content was authored and verified by the human authors. We accept full responsibility for all content in this paper.

## B METHODS

**Method Overview** We study the synergy between the data produced by our method when a modest *generalist* VLA serves as the prior policy. The premise is that, if we exploit the base policy’s prior correctly, it can both *solve hard tasks quickly* and *explore efficiently*. While recent work explores direct RL fine-tuning of expressive policy class (Mark et al., 2024; Dong et al., 2025b), such a formulation can be resource-intensive even for single-task tuning: e.g., OpenVLA-OFT requires per-GPU memory up to  $\sim 62.5$  GB for LIBERO training at batch size 8 (Kim et al., 2025). Meanwhile, it remains unclear whether these approaches scale gracefully to multi-task fine-tuning under heterogeneous setups. We therefore opt for a *decoupled* pipeline. We freeze the base policy  $\pi_b$  and learn a lightweight residual action policy  $\pi_\delta$  with sample-efficient off-policy RL (Gaussian policy parameterization). We then *collect expert data* by letting the residual “take over” after specified steps of “base policy probing”. Finally, we *distill* these skills back into the base model via SFT and deploy the generalist on diverse manipulation tasks. We provide the overview of PLD in Figure 4.

### B.1 DATA EFFICIENT RL VIA POLICY PRIOR WARM-START

Building upon the previous success of sample-efficient RL with prior data (Ball et al., 2023), we consider an off-policy actor-critic framework and maintain two separate buffers for offline and online experience replay. We first fill the offline buffer with successful rollouts  $\mathcal{B}_{offline} = \{\tau_1, \tau_2, \dots\}$  from the base policy  $\pi_b$ . This process serves as an importance sampling to preserve only the successful attempts. During training, the offline and online experiences will be replayed symmetrically; for example, mini-batches consist of equal samples from both buffers, ensuring that the value function is constantly trained on high-value state-action pairs.

In practice, we train a task-specific residual action module  $\pi_\delta(\cdot|s, a_b)$  conditioned on  $a_b \sim \pi_b$ . We use  $\pi_\delta$  to explore near the base policy behavior, actively searching for more optimal solutions guided by the Q-function. To modulate exploration and avoid deviating drastically from  $\pi_b$  during the initial phase, the delta action’s magnitude is scaled down to  $[-\xi, \xi]$ , where  $\xi \in [0, 1]$  is tuned by a scheduler. This design choice is two-fold: First, although unable to perfectly generalize to an unseen manipulation task or scenario, the base policy can make reasonable attempts to solve the task, serving as a useful initialization for exploration. Moreover, directly training the expressive foundation policy (e.g., flow action heads) to maximize the Q-value can be extremely difficult (Mark et al., 2024). In contrast, a residual Gaussian policy can be easily trained through any off-the-shelf off-policy RL algorithm.

Alongside  $\pi_\delta$ , action value function  $Q^{\bar{\pi}}$  acquired through policy iteration and TD-learning Sutton & Barto (2018) as in Eq. equation 1, where  $\bar{\pi}(\cdot|s) = \pi_b(\cdot|s)\pi_\delta(\cdot|s, a_b)$  is the combined policy.

$$Q^{\bar{\pi}}(s_t, \bar{a}_t) \leftarrow r(s, a) + \gamma \mathbb{E}_{s_{t+1} \sim p(\cdot|s_t, \bar{a}_t)} [Q^{\bar{\pi}}_{target}(s_{t+1}, \bar{a}_{t+1})], \bar{a} = a_b + a_\delta \quad (1)$$

To stabilize off-policy learning and mitigate forgetting, we introduce a warm-up stage using solely  $\pi_b$  for data collection akin to (Zhou et al., 2024b). Meanwhile, the Q-function is initialized by a conservative objective such as Cal-QL (Nakamoto et al., 2024). Importantly, we do not explicitly enforce behavior constraints to policy loss, such that the resulting expert  $\bar{\pi}$  is less influenced by either data quality or base policy performance.

## B.2 BOOTSTRAPPING RL SPECIALIST FOR SCALABLE DATA GENERATION

We then turn to the question of how to collect demonstration data using RL specialists. Data collected through RL experts is highly optimal, with consistent behavior and nearly no hesitation, demonstrating smooth solutions that finish tasks with a shorter horizon. However, such a narrow distribution of unimodal expert behavior may leave out-of-distribution and failure states underrepresented. Thus, scaling purely expert data may not result in a performance gain, but instead risks the generalist overfitting on these data and harming both robustness and generalization (As discussed in the following section).

To mitigate this issue, we propose a hybrid data collection scheme that incorporates base-policy initialization: We first rollout the base policy for random steps, then let the learned residual RL policy to take over, resulting in demonstration trajectories  $\tau_{demo} = \{(s_1, a_{b,1}), \dots, (s_{t-1}, a_{b,t-1})\} \cup \{(s_t, a_{b,t} + \bar{a}_t), \dots\}$  that contain the behavior of the expert recovering from a potential suboptimal region. We refer to this procedure as **base policy probing**. Accordingly, we boost the robustness of the RL expert by training the RL expert on an initial state distribution  $s_0 \sim p_0^{\pi_b}$  given by random steps of base policy probing. The probing step only serves as state initialization and will not be added to the replay buffer. The details of **PLD** are summarized in Algorithm 1.

## B.3 HOW DOES **PLD** WORK?

We take a deeper look at the underlying reason for **PLD** data’s bonus in generalization. As shown in Figure 10, we plot 50 trajectories for each method (task description: “open middle drawer of the middle cabinet”). RL expert provides optimal and concentrated solutions to the task, but lacks diversity and diverges far from the behavior of the base policy, while **PLD** data are clustered near the trials of the base policy and contain various recovery behaviors. Based on empirical observation, we hypothesize that due to the base policy probing, **PLD** data provides a solution that is biased towards the base policy, thus fine-tuning forgets less of the base model’s generalizability. This resembles observations in LLM fine-tune (Shenfeld et al., 2025), where the KL-divergence can serve as an indicator of forgetting. Meanwhile, large data coverage also benefits robustness in sequential decision making (Kelly et al., 2019).

## C EXTENSIVE RELATED WORKS

**Robotics Foundation Models** Following the success of large language models and vision language models (Brown et al., 2020; Touvron et al., 2023; Chen et al., 2022), recent works on robotics foundation models turned to a similar transformer-based architecture with aggressive data scaling.

This inspired earlier works in VLAs such as RT-1, RT-2, and OpenVLA, etc. (Brohan et al., 2023b;a; Kim et al., 2024; Xue et al., 2025). Meanwhile, diffusion-based action generation, explored in Chi et al. (2024), takes motivation from generative modeling techniques (Ho et al., 2020), demonstrating smooth and accurate action generation. This has led to more recent VLA architectures to-date, such as Octo (Team et al., 2024), OpenVLA-OFT (Kim et al., 2025), GR00T (Bjorck et al., 2025), and the  $\pi$ -series of models (Black et al., 2024; Intelligence et al., 2025; Pertsch et al., 2025). The VLA training procedure is typically analogous to VLM training. First, model weights are initialized from the respective VLM backbones (Kim et al., 2024; Black et al., 2024). Then, the model is supervised with next-token-prediction tasks on diverse pretraining datasets, spanning across multi-modal web data (Intelligence et al., 2025) such as COCO (Chen et al., 2015) and VQAv2 (Goyal et al., 2017), and robotics-specific, cross-embodiment data (Khazatsky et al., 2025; O’Neill et al., 2024). Finally, supervised fine-tuning is conducted on a small set of high-quality teleoperation data collected from the target robot deployment platform performing the target tasks.

**Sample-efficient RL with Data and Policy priors** Sample and exploration efficiency have been a long-standing problem in RL, especially in sparse-reward settings. Recent works have explored leveraging offline data to improve sample efficiency. Offline-to-online transfer (Vecerik et al., 2017; Nair et al., 2020; Kostrikov et al., 2021; Nakamoto et al., 2024; Zhou et al., 2024b; Li et al., 2025) considers a two-stage pipeline that first initializes policy or critic using pessimism or constrained objective in offline RL (Levine et al., 2020) and follows with an online fine-tuning phase to have new data collected and alleviate distributional shift; Hybrid RL (Song et al., 2022, 2024; Ball et al., 2023) considers online RL with access to an offline dataset. Given expert demonstration, one can either continuously replay this data to ensure high-value state visitation (Ball et al., 2023) or to guide exploration (Dong et al., 2025a). Data prior can also guide reset-free real-world learning (Walke et al., 2023; Sharma et al., 2023). Another line of work assumes access to policy prior, such as a pre-trained generalist. Ye et al. (2023); Chen et al. (2025); Jülg et al. (2025) leverage foundation policy to guide RL through an auxiliary behavior regularization objective. Action editing is another efficient way to improve upon the policy prior. ResiP (Ankile et al., 2025) considers learning a residual policy through PPO (Schulman et al., 2017), while EXPO (Dong et al., 2025b) considers an off-policy solution and co-trains the base policy during the process. Our work leverages a suboptimal base policy to achieve a non-zero success rate for warm-starting exploration, but does not require access to oracle demos or a human expert for further intervention.

**VLA post-training** The prevailing large-scale recipe for VLA post-training is to *pretrain* on diverse, heterogeneous robot data and then *fine-tune* on task-specific demonstrations (Zhou et al., 2024a; Black et al., 2024). For example, Black et al. (2024) performs supervised post-training on a carefully curated task-targeted corpus, with per-task coverage ranging from a few to over 100 hours of teleoperation. Because such post-training data are expensive to acquire, the authors note that most diversity must come from the pretraining mixture—underscoring a key limitation of pure SFT: data scarcity and limited coverage at adaptation time. To enable self-improvement, prior work has explored scaling high-quality data via *online RL specialists* (Ball et al., 2023). However, these pipelines often require substantial human intervention and collect data in a large way *agnostic* to the generalist’s behavior, restricting scalability. Other lines investigate *on-policy* RL for post-training (Lu et al., 2025; Tan et al., 2025), or optimize *single-task* fine-tuning at the expense of generalization (Chen et al., 2025). Our work jointly targets these limitations by seeking a post-training pipeline that reduces human effort, aligns data collection with the generalist’s state distribution, and remains sufficiently sample efficient for real-world systems.

**RL with Residual Actor** Residual actors are lightweight policies that output adjustments on top of the base policy’s action. Compared to the expressive base policy, the residual actor reduces optimization complexity, circumventing problems regarding computation inefficiency or unstable training dynamics of large models or flow-based policies (Mark et al., 2024; Tan et al., 2025).

Residual RL has been leveraged to address different challenges in robotics. (Haldar et al., 2023) Consider data-efficient imitation refinement to adapt the base policy across robot morphologies and new object configurations; (Yu et al., 2023) bridges embodiment or modality gaps, such as human-hand to robot-gripper transfer or tactile/vision modality mismatches; (Ankile et al., 2025) scales to long-horizon or precision tasks, augmenting a frozen action chunking policy with a residual policy to address the distribution shifts and the lack of closed-loop corrective control. They include the

residual policy as a core component at test time and the training process is limited to simulation and requires sim2real transfer. (Dong et al., 2025b) leverages a residual actor to address the challenge of fine-tuning expressive policies. The small Gaussian policy can be seamlessly optimized using existing off-policy RL to maximize the Q function. Then expressive base policy can match the edit policy’s behavior using the imitation objective. In contrast, one of the core motivations for adopting residual RL in this work is to enhance sample efficiency. Residual policy with controlled scale enables exploration that starts from the base policy’s trails. Along with other design choices, our method can be directly adopted for real-world learning on physical robot hardware. Also, we consider augmenting the base policy by distilling expert behavior.

## D ALGORITHM

---

### Algorithm 1 PLD with base-policy initialization

---

**Require:**  $\pi_b, \pi_\delta, Q_\phi, Q_{\phi'}, \alpha, \gamma, \mathcal{B}_{\text{offline}}, \mathcal{B}_{\text{online}}$

**# Initialization**

Collect  $n$  successful trajectories of  $\pi_b$ :  $\mathcal{D}_{\text{offline}} = \{\tau_1, \tau_2, \dots, \tau_n\}$

Initialize online buffer  $\mathcal{D}_{\text{online}} = \emptyset$

Initialize the critic network  $Q_\phi, Q_{\phi'}$  with Cal-QL on  $\mathcal{D}_{\text{offline}}$

Randomly initialize delta policy network  $\pi_\delta$

**# RL training**

Freeze  $\pi_b$ , denote  $\bar{\pi}(\cdot|s) = \pi_b(\cdot|s)\pi_\delta(\cdot|s, a_b)$

**for** each RL step **do**

**if** collect data **then**

**if** Warm up step **then**

      base model rollout  $a \sim \pi_{\text{base}}(\cdot|s)$

**else**

      sample action  $\bar{a} \sim \bar{\pi}(\cdot|s)$

**end if**

    Environment step:  $r, s', done = env.step(\bar{a})$

    Add  $(s, a, \mu, r, s')$  to buffer  $\mathcal{D}_{\text{online}}$ .

**end if**

  Equally sample data from online and offline buffer:  $b \sim \mathcal{D}_{\text{online}} \cup \mathcal{D}_{\text{offline}}$

  Calculate TD target by bootstrapping  $\bar{\pi}$

  Update  $Q_\phi$  by equation 1

  Update  $\pi_\delta$  by maximizing the SAC target

**Polyak update**  $\phi' = \rho\phi' + (1 - \rho)\phi$

**end for**

**#Base policy SFT**

For each task, we collect hybrid behavior dataset  $\mathcal{D}_{\text{SFT}}$ :

$$\pi(s_t) = \begin{cases} a_{\text{base}}, & t < T_{\text{base}} \\ a_{\text{base}} + a_\delta, & t \geq T_{\text{base}} \end{cases}$$

**for** each SFT step **do**

  update  $\pi_b$  by BC objective.

**end for**

Return  $\pi_b$

---

## E MORE RESULTS

### E.1 IN-DISTRIBUTION PERFORMANCE

In this section, we investigate how effectively the proposed pipeline enhances the performance of the VLA. We evaluate in-distribution fine-tuning on the LIBERO benchmark using three subsets, each consisting of 10 language-conditioned tasks: *LIBERO-Object*, *LIBERO-Spatial*, and *LIBERO-Goal*. We additionally report results on a custom suite that consists of 4 tasks from SimplerEnv. To

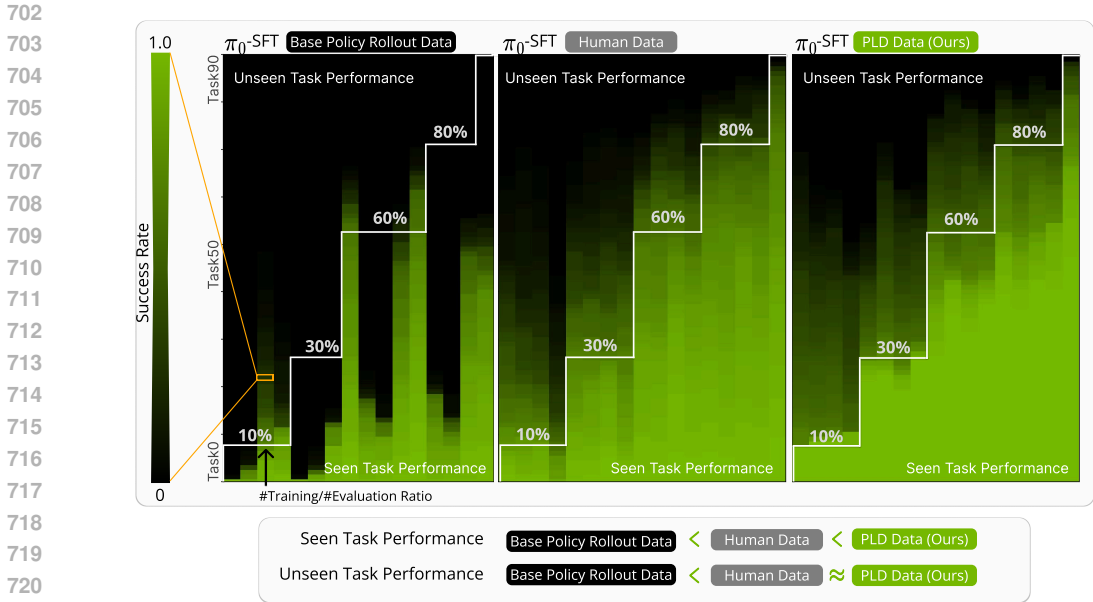


Figure 5: **Synergetic effect of PLD data.** We fine-tune  $\pi_0$  on subsets of LIBERO-90 with varying **task coverage ratios**, where each ratio (10–80%) indicates the fraction of distinct task instances included in training relative to the full 90-task distribution. For each ratio, we randomly sample 4 disjoint subsets of tasks and report the average results. The x-axis thus represents the degree of task coverage (not the number of trajectories), while the evaluation is always conducted on all 90 tasks. We compare different data formulations: **PLD** data yields the highest in-distribution performance while retaining the cross-task generalization property of high-quality human data. It further enables modest-level zero-shot transfer even when trained on only 10% of tasks (24.4% SR on unseen tasks), whereas the VLA fine-tuned on base-policy rollout data (0-1 REINFORCE) underperforms and fails to generalize. (Success rate numbers are reported in Table 1.)

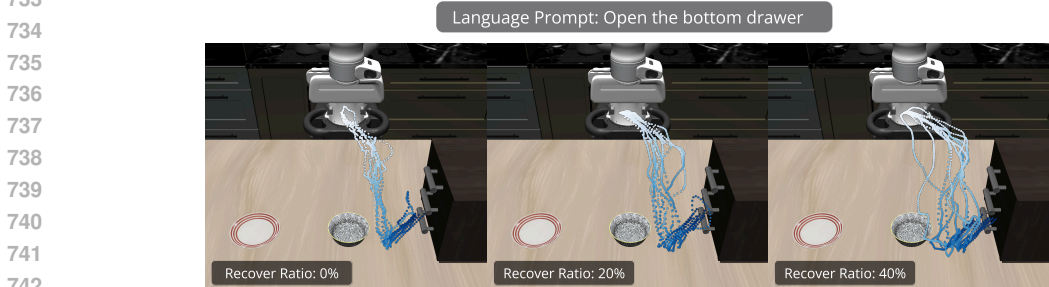


Figure 6: **Visualization of Data diversity.** We visualize **PLD** data with different base policy initialization probing horizons. Increasing probing horizon yields longer episodes and greater diversity among successful trials. This broader data support leads to improved fine-tuning performance, which eventually saturates. (As the saturation curve shown in Figure 14).

demonstrate architecture-agnosticism, we instantiate the base VLA with (i) **OpenVLA** (autoregressive action tokens) (Kim et al., 2024) and (ii)  $\pi_0$  (flow-matching action head) (Black et al., 2024). Since VLA models are mainly trained on real-world datasets that cannot work out of the box on simulation benchmarks, we leverage their official checkpoints for model fine-tuning on each benchmark as the baseline. At test time, each policy is evaluated on 50 episodes per task, and we report the mean success rate per suite and average over the benchmark. Table 3 and Table 2 list the performance gain achieved by further applying our method. Across all suites and both architectures, **PLD** data yields consistent absolute gains over human-only SFT while requiring *no additional human*

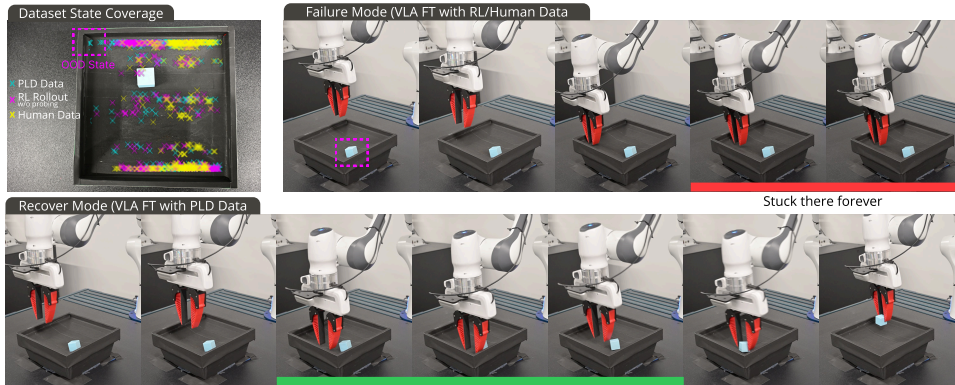


Figure 7: Visualization of failure mode and recovery behavior in the real-world.

Table 1: LIBERO-90 Success rate for  $\pi_0$  SFT with different dataset.

PLD Data			Base Policy Rollout Data			Human Data		
Ratio	Overall SR	Seen/Unseen SR	Ratio	Overall	Seen/Unseen	Ratio	Overall	Seen/Unseen
0.1	0.314	0.941	0.1	0.103	0.523	0.1	0.272	0.796
		0.244			0.056			0.214
0.3	0.470	0.968	0.3	0.068	0.198	0.3	0.419	0.829
		0.259			0.015			0.240
0.6	0.637	0.872	0.6	0.328	0.506	0.6	0.611	0.829
		0.283			0.062			0.286
0.8	0.745	0.864	0.8	0.344	0.423	0.8	0.694	0.803
		0.268			0.031			0.256
1.0	0.871	0.871	1.0	0.488	0.488	1.0	0.815	0.815
		N/A			N/A			N/A

demonstrations. We observe that larger PLD datasets monotonically improve in-distribution success and that the distilled generalist notably surpasses the average specialist, indicating effective transfer of task-specific competence into the base VLA.

## E.2 OCTO SFT FOR SIMPLERENV TASKS

In addition to the in-distribution results on LIBERO, we provide results on SimplerEnv in Table 2. Similar to the training and evaluation protocol on LIBERO, we first train task-specific residual RL specialists and fine-tune VLA on PLD data for all four tasks.

## E.3 GENERALIZE TO LONG-HORIZON TASK

We assess skill composition on LIBERO-100 by fine-tuning the base VLA on LIBERO-90 (source) and evaluating zero-shot on the held-out LIBERO-10 long-horizon tasks (target). To construct PLD data, we first train residual RL specialists independently on each LIBERO-90 task, then aggregate their successful rollouts. As shown in Figure 9, the fine-tuning of the data PLD exceeds the tuning of the data from the baseline policy roll-out (self-bootstrapped), but still falls short of the performance achieved with demonstrations by human experts.

# F IMPLEMENTATION

## F.1 RL BASELINES

To ensure an apple-to-apple comparison in Section 3.1, we implement these baselines based on the SERL Luo et al. (2024) framework and adapt them to fit in the settings of our study. We provide a detailed explanation of baseline formulation and our implementation. As for the hyperparameter

**RLPD** RLPD (Ball et al., 2023) proposed a hybrid RL pipeline that leverages offline data to foster learning in challenging sparse reward settings. During training, it equally draws samples from both

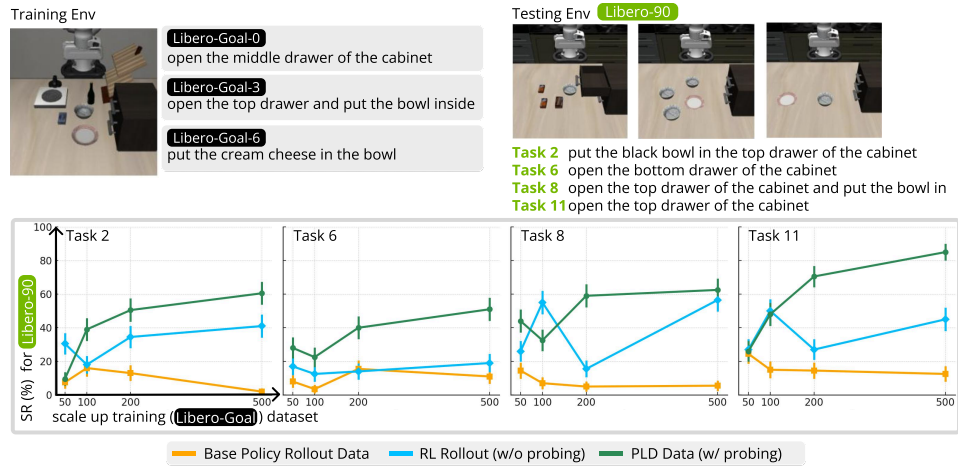


Figure 8: **Few-shot generalization.** Scaling in-distribution (LIBERO-goal) **PLD** yields better few-shot performance on new tasks (LIBERO-90).

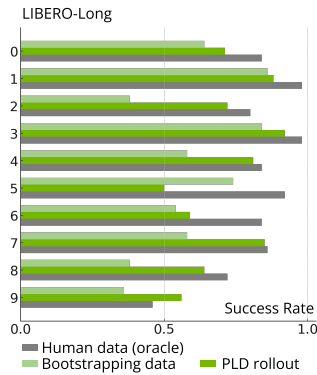


Figure 9: **Short-to-long generalization.** Zero-shot evaluation on LIBERO-10 long horizon tasks.

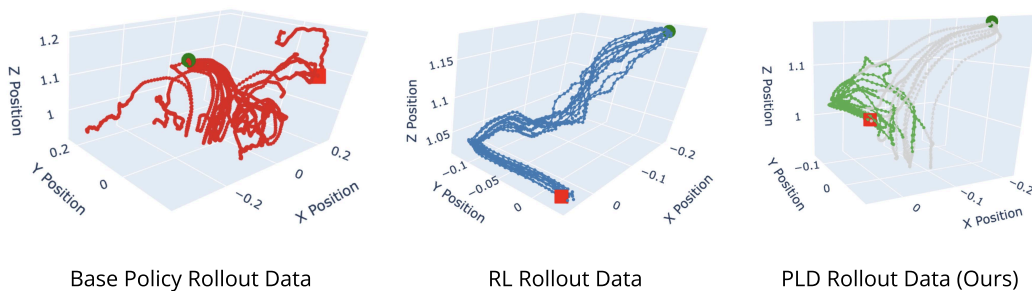


Figure 10: **Visualization of different data sources.** We plot 50 trajectories for each method (task prompt: “open middle drawer of the middle cabinet”). RL expert data is of high quality but lacks diversity and diverges far from base policy behavior, while **PLD** data aligns better with the base policy and contains diverse recovery behavior.

Table 2: Evaluate **PLD** on SimplerEnv

Model	WidowX Pick Eggplant	WidowX Pick Carrot	Google Open Drawer	Google Coke Can	Avg
Octo-SFT	65.5	43.3	92.5	85.7	71.8
<i>w/ ours</i>	97.8	93.9	99.3	95.5	96.6
$\Delta$	+32.3	+50.6	+6.8	+9.8	+24.9

Table 3: Performance on LIBERO benchmark of VLA models fine-tuned on **PLD** data.

Model	$\pi_0$				OpenVLA			
	Spatial	Object	Goal	Avg	Spatial	Object	Goal	Avg
Baseline (SFT/OFT)	95.2	97.6	87.4	93.4	92.9	99.1	83.25	91.8
<i>w/ PLD</i>	<b>97.7</b>	<b>98.5</b>	<b>95.3</b>	<b>97.2</b>	<b>99.5</b>	<b>99.1</b>	<b>98.9</b>	<b>99.2</b>
$\Delta$	+2.5	+0.9	+7.9	+3.8	+6.6	+0.0	+15.7	+7.4

the online and offline buffer. It also uses LayerNorm to deal with the Q-value blow-ups common when querying OOD actions under a high up-to-date (UTD) ratio. We refer to the implementation in the SERL software for both simulation and real deployment.

**WSRL** In the original paper (Zhou et al., 2024b), WSRL uses Cal-QL (Nakamoto et al., 2024) to pre-train both the action and critic during the offline phase. For the online phase, it discards offline data and warms up the replay buffer with 50k steps of pre-trained policy rollouts. We did not provide a large dataset that contains diverse behavior as on the D4RL (Fu et al., 2020) benchmark. Rather, we use the same procedure as **PLD** to collect successful trajectories from the base model. We implement WSRL under the SERL framework, as the UTD is no longer fixed to 4. This baseline can be considered as an ablation of the residual policy and offline data replay. We use the WSRL baseline as an ablation study of the warm-up online exploration using the base policy, and offline data retention through hybrid data replay.

**JSRL** Jump-start RL (Uchendu et al., 2023) is a meta-algorithm using an existing guide policy to “rolling-in”. The key mechanism is to shape the initial-state distribution for the learner: JSRL repeatedly resets episodes from states that the guide visits (a curriculum from easy/near-goal states to harder/far-from-goal states), making difficult tasks learnable with fewer trials. It leverages the guide policy for data collection, without directly imitating its actions. JSRL is agnostic to the underlying RL backbone. In practice, we choose SAC to learn the exploration policy. Since JSRL only leverages the policy prior (VLA policy in practice) to warm-up exploration during online interaction, we use it as an ablation of the hybrid experience replay mechanism.

**Cal-QL** Calibrated Q-learning (Nakamoto et al., 2024) addresses the underestimation issue of CQL (Kumar et al., 2020), thereby significantly improving fine-tuning performance in the offline-to-online setting. It learns a conservative value function that underestimates the value of OOD actions, while ensuring the values are within a reasonable scale. In practice, it under-bounds the conservative Q function by the value of the behavior policy  $\mu$  (policy corresponds to the offline dataset  $\mathcal{D}$ ). The modified Q-learning objective is the following:

$$\min_{\theta} \alpha (\mathbb{E}_{s \sim \mathcal{D}, a \sim \pi} [\max(Q_{\theta}(s, a), V^{\mu}(s))] - \frac{1}{2} \mathbb{E}_{s, a \sim \mathcal{D}} [(Q_{\theta}(s, a) - \mathcal{B}^{\pi} \bar{Q}(s, a))^2])$$

Where  $\bar{Q}$  is the target Q-value function and the second term corresponds to minimizing TD-error Lillicrap et al. (2015).

**Implicit Q-Learning (IQL).** IQL is an in-sample offline RL method that avoids querying  $Q$  on out-of-distribution actions while still improving over the behavior policy (Kostrikov et al., 2021). The key step is to fit a *state value*  $V_{\psi}$  by *expectile regression* over the actions of the dataset and then bootstrap  $Q_{\theta}$  toward this value. Let  $\delta(s, a) = Q_{\theta}(s, a) - V_{\psi}(s)$  and define the expectile loss

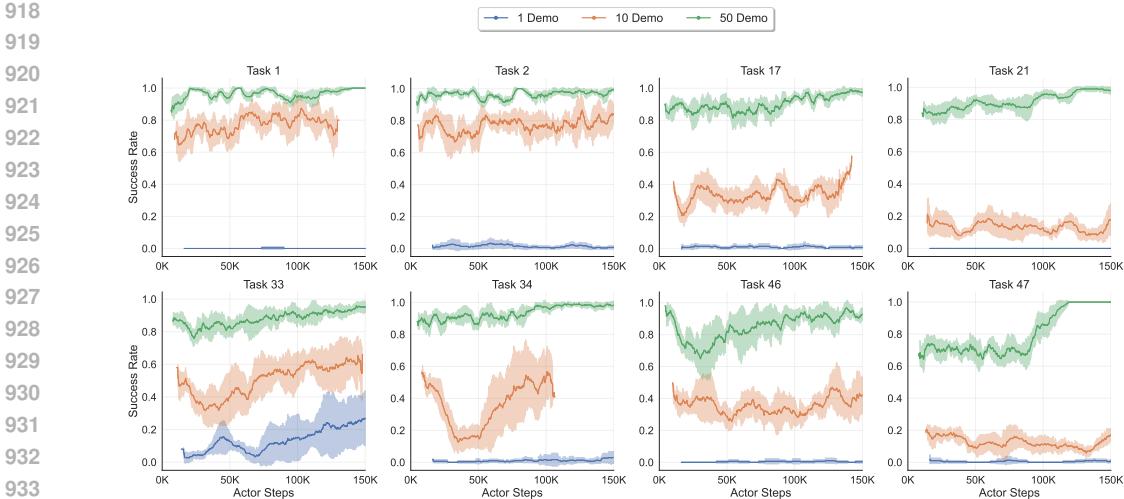


Figure 11: **Base policy ablation.** Mean and 95% CIs of rollout performance across 6 seeds.

$\mathcal{L}_\eta(\delta) = |\eta - \mathbf{1}\{\delta < 0\}| \delta^2$  with  $\eta \in (0.5, 1)$ . IQL alternates

$$(V) \quad \min_{\psi} \mathbb{E}_{(s,a) \sim \mathcal{D}} [\mathcal{L}_\eta(Q_\theta(s, a) - V_\psi(s))], \quad (2)$$

$$(Q) \quad \min_{\theta} \mathbb{E}_{(s,a,s') \sim \mathcal{D}} [(Q_\theta(s, a) - (r + \gamma V_\psi(s')))^2], \quad (3)$$

$$(\text{policy}) \quad \max_{\phi} \mathbb{E}_{(s,a) \sim \mathcal{D}} \left[ \exp\left(\frac{Q_\theta(s,a) - V_\psi(s)}{\beta}\right) \log \pi_\phi(a | s) \right], \quad (4)$$

which realizes policy improvement without out-of-distribution action queries (the policy step reduces to advantage-weighted regression) (Kostrikov et al., 2021). In our comparison to *Cal-QL* (Nakamoto et al., 2024) as a critic-initialization baseline, we consider a simplified version of IQL that *directly* regresses  $Q_\theta$  toward an  $n$ -step return  $R_t = \sum_{i=t}^{t+n-1} \gamma^{i-t} r_i + \gamma^n V_\psi(s_{t+n})$  using expectile regression:

$$\min_{\theta} \mathbb{E}_{(s_t, a_t) \sim \mathcal{D}} [\mathcal{L}_\eta(Q_\theta(s_t, a_t) - R_t)].$$

Unless otherwise noted, we set  $\eta = 0.7$ , a value shown to propagate high-value signals effectively in the IQL paper.

## F.2 DESIGN CHOICES OF **PLD**

In this section, we provide a detailed study of design choices that make **PLD** data efficient and achieve high convergence performance. We evaluate all algorithms on the selected 8 LIBERO-90 tasks.

**Sensitivity to Base Model Performance.** We evaluate how the quality of the base model influences the efficacy of the RL phase in **PLD**. Using a subset of 8 tasks from LIBERO-90, we fine-tune the initial policy  $\pi_0$  using 1, 10, and 50 demonstrations, yielding three distinct baselines:  $\pi_0^{1 \text{ demo}}$ ,  $\pi_0^{10 \text{ demo}}$ , and  $\pi_0^{50 \text{ demo}}$ . We then apply Phase 1 of **PLD** to each baseline. For the experimental setup, we perform a hyperparameter sweep over action scales  $\{0.01, 0.1, 0.5, 1.0\}$  across 6 random seeds, reporting the average performance of the best configuration. As shown in Figure 11, residual RL is highly effective when initialized with a competent policy, boosting success rates to 99% provided the base model achieves at least 80% success. Conversely, the method struggles when the base model is too weak; for example, with  $\pi_0^{1 \text{ demo}}$ , residual RL fails to converge on 7 out of 8 tasks.

**Sensitivity to the initialization horizon** We choose task 0-9 from LIBERO-90, change the steps we used to initialize the random sample, initiating steps  $T_{\text{base}} \sim [0, \alpha T]$  to rollout the base policy.  $\alpha \in [0.0, 0.2, 0.4, 0.6, 0.8]$ . As  $\alpha$  increases, the average episode length of successful trajectories increases, indicating a detour required to correct the suboptimal behavior of the base policy. As

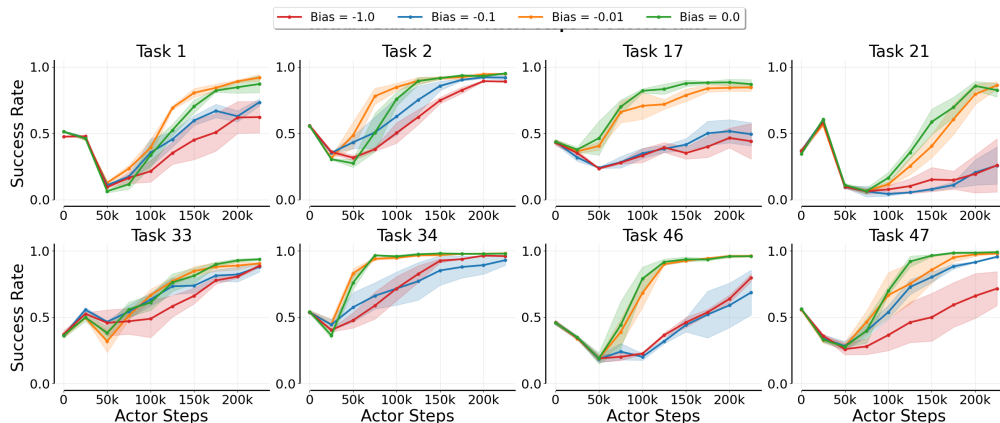


Figure 12: **Reward bias ablation.** Mean and 95% CIs of rollout performance across 3 seeds.

demonstrated in Figure 14, performance plateaus at  $\alpha = 0.6$  and drops as  $\alpha$  increases further. This is consistent with our analysis that SFT benefits from the data diversity.

**Reward shaping** We empirically analyze the impact of naive reward shaping. Specifically, we consider a step-wise *survival cost* as reward bias as in prior works Luo et al. (2024). As shown in Section F.2, adding a slight reward bias has little impact, but it could increase convergence speed in 2 out of 8 tasks; However, A large bias could significantly hinder performance. For the major results reported in the main paper, we do not apply reward shaping.

**Action scale** One core component of residential policies is the scale of exploration. To avoid un-learning results from diverging too far from the base policy, delta actions are usually scaled down and bounded within a range of  $[-\xi, \xi]$  (Ankile et al., 2025; Dong et al., 2025b). Figure 13 compares different residual action scales. Setting  $\xi$  too large at the start can degrade early performance: updates deviate excessively from the base policy, inducing unstable exploration, while a small  $\xi$  will lead to insufficient exploration and lower asymptotic performance. We argue that  $\xi$  needs to be carefully tuned to enable exploration while minimizing performance drop. For single-arm manipulation, we suggest  $\xi = 0.5$  a good choice for LIBERO and  $\xi = 0.1$  for SimplerEnv.

**Critic pre-training** While warm-start through pre-training the critic is beneficial to asymptotic performance and prevents initial performance drop, the careful selection of the pre-training method could be important as well. We compare using CQL, Cal-QL, and IQL to the pre-training method. We consider using only 50 trajectories of successful trials of the base policy, while the standard offline RL benchmark tends to have far larger data volume (Fu et al., 2020). In Figure 15, online performance using the Cal-QL pre-trained critic is consistently better and is robust to the conservative coefficients  $\alpha$ . CQL demonstrates the worst performance with a severe forgetting issue, which aligns with the previous study (Nakamoto et al., 2024).

1026  
 1027  
 1028  
 1029  
 1030  
 1031  
 1032  
 1033  
 1034  
 1035  
 1036  
 1037  
 1038  
 1039  
 1040  
 1041  
 1042  
 1043  
 1044  
 1045  
 1046  
 1047  
 1048  
 1049  
 1050  
 1051  
 1052  
 1053  
 1054  
 1055  
 1056  
 1057  
 1058  
 1059  
 1060  
 1061  
 1062  
 1063  
 1064  
 1065  
 1066  
 1067  
 1068  
 1069  
 1070  
 1071  
 1072  
 1073  
 1074  
 1075  
 1076  
 1077  
 1078  
 1079

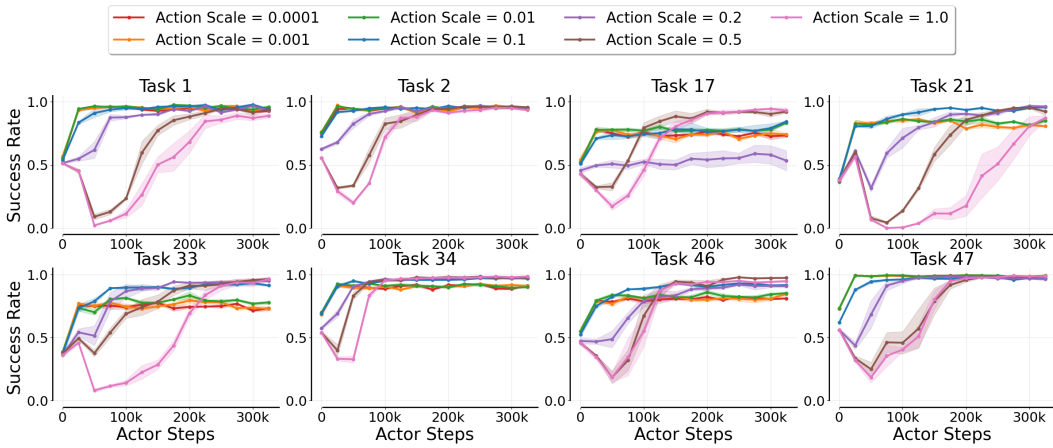


Figure 13: **Action scale ablation** Mean and 95% CIs of rollout performance across 3 seeds.

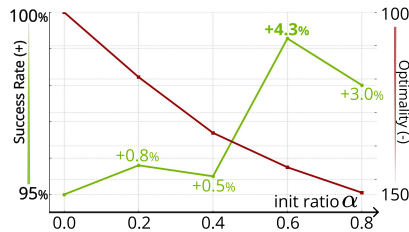


Figure 14: **Ablation of Probing Horizon.** With  $\alpha$  measuring the percentage of base policy probing during data collection, we see fine-tune performance plateau at  $\alpha = 0.6$ . Performance drops monotonically as  $\alpha$  increases further.

1080  
 1081  
 1082  
 1083  
 1084  
 1085  
 1086  
 1087  
 1088  
 1089  
 1090  
 1091  
 1092  
 1093  
 1094  
 1095  
 1096  
 1097  
 1098  
 1099  
 1100  
 1101  
 1102  
 1103  
 1104  
 1105  
 1106  
 1107  
 1108  
 1109  
 1110  
 1111  
 1112  
 1113  
 1114  
 1115  
 1116  
 1117  
 1118  
 1119  
 1120  
 1121  
 1122  
 1123  
 1124  
 1125  
 1126  
 1127  
 1128  
 1129  
 1130  
 1131  
 1132  
 1133

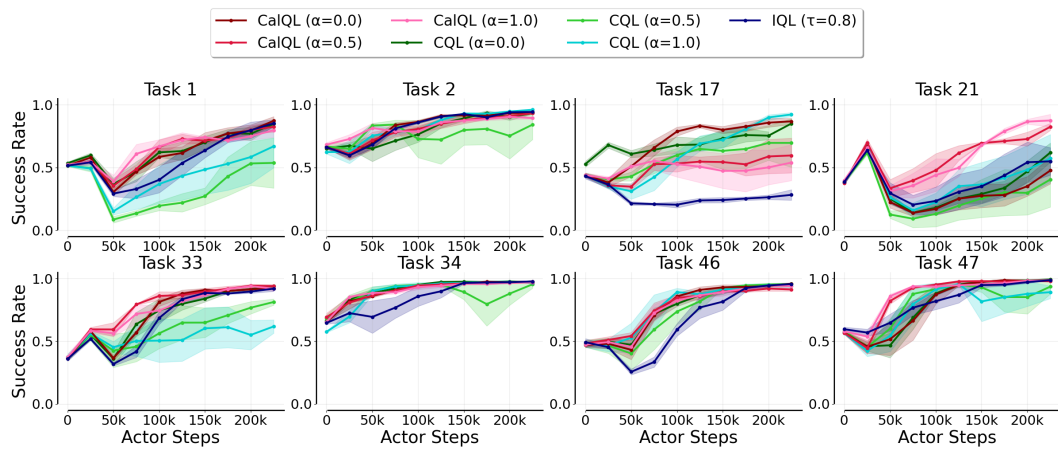


Figure 15: **Offline pre-training ablation.** Mean and 95% CIs of rollout performance across 3 seeds.

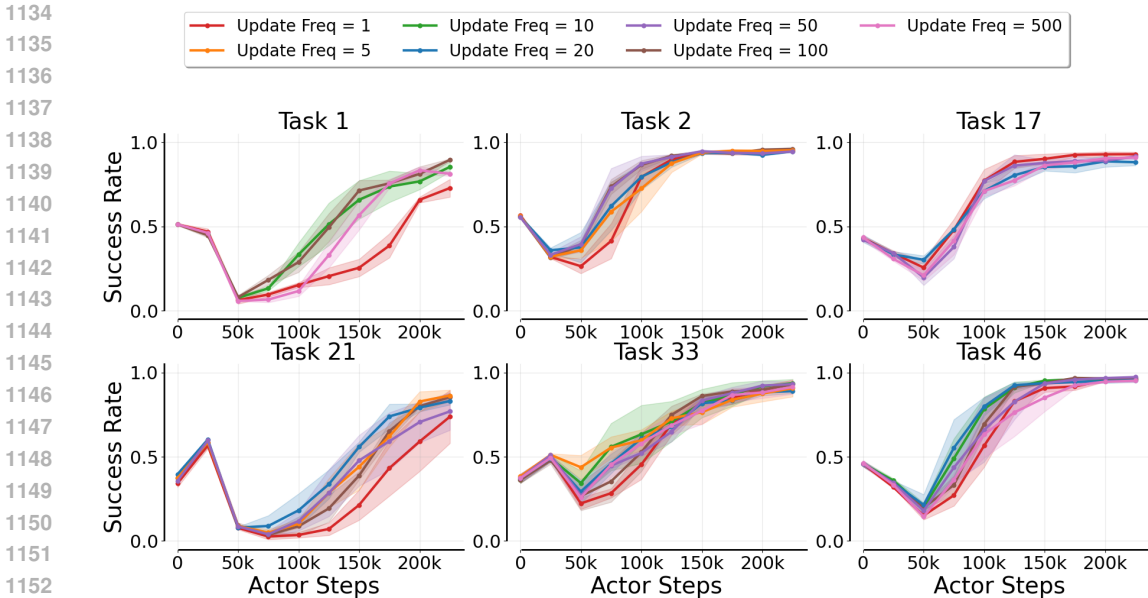


Figure 16: **Update frequency ablation.** Mean and 95% CIs of rollout performance across 3 seeds.

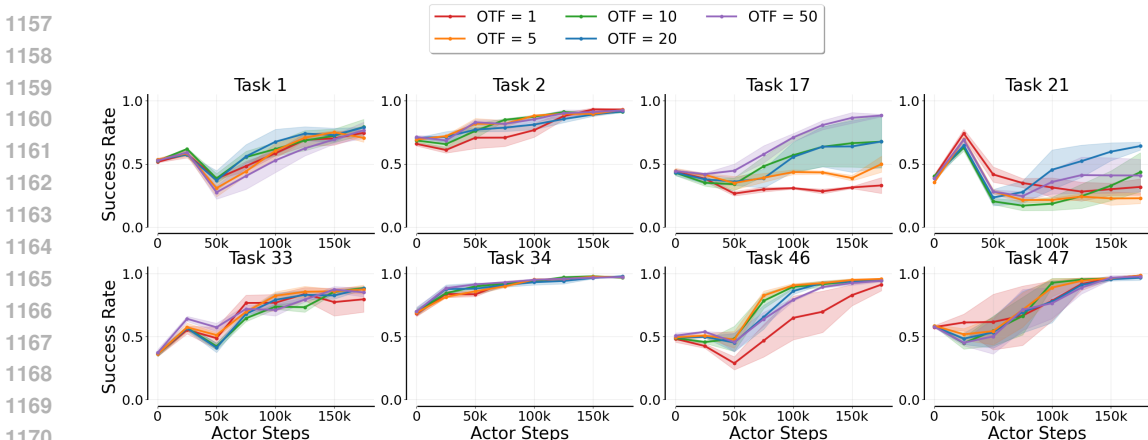


Figure 17: **On-the-fly Policy Ablation.** Mean and 95% CIs of rollout performance across 3 seeds.

**Update frequency** In the SERL pipeline, data collection and policy learning run asynchronously and periodically exchange network parameters and online data. We ablate the *update frequency*—the number of gradient steps performed by the learner between parameter synchronizations with the data-collection actor—sweeping from 1 to 500. As shown in Figure 16, overall performance is largely insensitive to this hyperparameter, indicating robustness across a wide range of synchronization cadences.

**On-the-Fly Policy** On-the-fly (OTF) policy is introduced in (Dong et al., 2025b) to more effectively maximize the value function. It samples multiple actions and backs up the maximum Q value during TD learning. We adopt OTF to **PLD** while only sampling multiple actions from the residual policy  $\pi_\delta$  and conditioned on a fixed base action. We compare different sample sizes in Figure 17. We found that OTF can improve sample efficiency, and a larger sample size ( $> 20$ ) shows significant performance gain. But empirically, the asymptotic performance will eventually be similar. We use OTF= 1 by default.

1188  
 1189  
 1190  
 1191  
 1192  
 1193  
 1194  
 1195  
 1196  
 1197  
 1198  
 1199  
 1200  
 1201  
 1202  
 1203  
 1204  
 1205  
 1206  
 1207  
 1208  
 1209  
 1210  
 1211  
 1212  
 1213  
 1214  
 1215  
 1216  
 1217  
 1218  
 1219  
 1220  
 1221  
 1222  
 1223  
 1224  
 1225  
 1226  
 1227  
 1228  
 1229  
 1230  
 1231  
 1232  
 1233  
 1234  
 1235  
 1236  
 1237  
 1238  
 1239  
 1240  
 1241

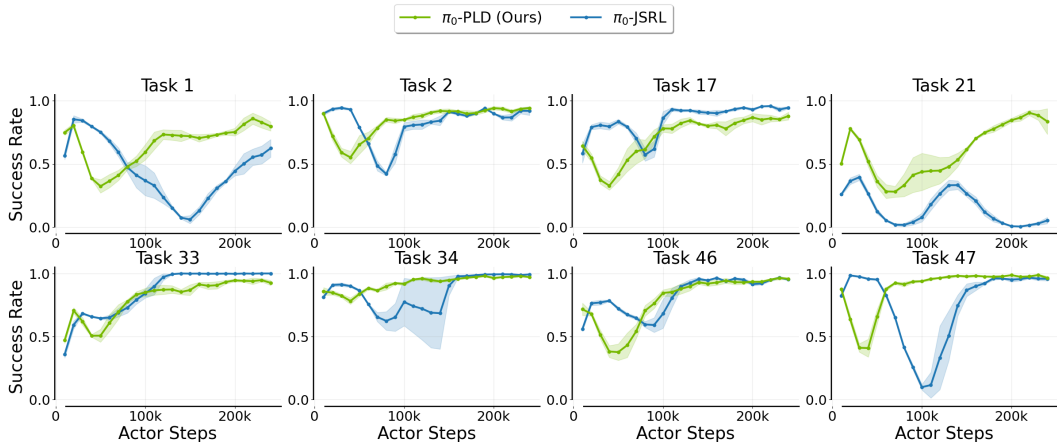


Figure 18: Compared with JSRL. Mean and 95% CIs of rollout performance across 3 seeds.

**JSRL** We further provide results, including JSRL Uchendu et al. (2023) in Figure 18. We modify the original implementation by opting for a linear scheduler. JSRL demonstrates high data efficiency in general, but could fail to converge on some tasks. While PLD can reliably provide solutions for all tasks.

## G IMPLEMENTATION DETAILS

### G.1 RL ALGORITHM

To ensure apples-to-apples comparisons, all baselines in Section 3.1 and Section F.2 use the same network architecture—an 3-layer MLP Gaussian policy and Clipped Double Q-networks (CDQ) Fujimoto et al. (2018) with LayerNorm (Ba et al., 2016). Both actor and critic use a pre-trained ResNetV1-10 encoder to extract visual information. We present a detailed hyperparameter setting in Table 4.

### G.2 COMPUTATIONAL COST ANALYSIS

We analyze the computational resources required for the Residual RL phase (Phase 1) of PLD, conducted on NVIDIA L40 GPUs for simulation and an RTX 4090 for real-world experiments. A key advantage of PLD is its resource efficiency: since the large VLA base policy remains frozen and we only optimize a lightweight residual MLP, the GPU memory footprint is significantly reduced compared to full fine-tuning. As shown in Table 5, training occupies a peak of only ~5GB VRAM per task. To further optimize GPU usage, we offload the experience replay buffer to System RAM (up to 100GB per task). This low GPU footprint enables linear scalability for multi-task learning; for example, we successfully parallelized the LIBERO-90 experiment by distributing 90 tasks across a cluster node with 90 L40 GPUs and 10TB of CPU memory.

### G.3 SFT

We employ LoRA (Hu et al., 2021) to fine-tune our VLA base models (OpenVLA and  $\pi_0$ ) efficiently. All SFT experiments are conducted on a node with 8x NVIDIA L40 GPUs. We use a LoRA rank of  $r = 32$  and apply the default hyperparameters provided by the respective open-source codebases for both  $\pi_0$  and OpenVLA.

### G.4 INFERENCE AND ACTION CHUNKING.

We adopt  $\pi_0$  model and Jax (Bradbury et al., 2018) implementation for real-world experiments, to handle high-frequency control in real-world tasks, we utilize temporal action chunking.

Table 4: RL hyperparameter settings. We share the same setting across all tasks.

Hyperparameter	Value
<b>Training</b>	
Batch size	256
Buffer capacity	250000
Discount factor ( $\gamma$ )	0.99
Gradient clipping norm	1.0
Learning rate	$3 \times 10^{-4}$
Optimizer	AdamW
Reward bias	0.0
<b>Residual Policy</b>	
Target entropy	$-\frac{act\_dim}{2}$
Initial temperature ( $\tau$ )	1.0
Action scale ( $\xi$ )	0.5
<b>Critic</b>	
Q functions esemble	2
Target update rate	0.005
<b>Architecture</b>	
Visual Encoder	ResNetv1-10
Hidden layer dimension	256
Latent space dimension	256
Q function drop out	0.0
Activation	Tanh
Normalization	LayerNorm

Table 5: **Computational Cost Analysis.** Resources reported are per single task.

Setting	Hardware	Peak VRAM	System RAM	Training Time
LIBERO (Sim)	NVIDIA L40	~5 GB	~100 GB	4-6 Hours
Real World	NVIDIA RTX 4090	~5 GB	~100 GB	2-8 Hours

- For standard Franka manipulation tasks, we use a chunk size of  $k = 20$  and an execution step of  $H = 6$  (inferencing every 6 steps to predict the next 20).
- For the YAM arm GPU insertion task, we increase the temporal context, using a chunk size of  $k = 26$  and an execution step of  $H = 15$ .

## H REAL-WORLD EXPERIMENTS

We deploy **PLD** on a 7-DoF Franka Emika Pand with end-effector delta pose control at 20 Hz. The robot is equipped with one wrist-mounted camera, one side-view camera, and proprioceptive sensing as inputs. For each task, we pretrain a independent binary reward classifier by collecting a small-scale dataset of success and failure states. The model structure follows the setup in (Luo et al., 2025), which use a pretrained ResNet-10 and a 3-layer MLP model. We ensure the trained

classifier using augmented false positive samples until it achieves 99% success rate for each task. Due to the 3D printed desk, we don’t need to reset the environment for the pick-cube task. **PLD** performs auto-reset, residual RL training, and SFT automatically without human supervision. For peg-insertion task (depicted in Figure 20), human need to randomly move the position of hole to increase diversity.

**Data collection and policy training.** We first collected 200 teleoperated trajectories to perform supervised fine-tuning (SFT) of the base policy  $\pi_0$ . Using this initialization, we trained  $\pi_0$ -**PLD** and  $\pi_0$ -RLPD without human interventions. Both policies reached 100% success on the two tasks within 2 hours of training. We then leveraged the learned expert policies to autonomously collect 200 successful demonstrations each, forming datasets  $\mathcal{D}^{\text{PLD}}$  and  $\mathcal{D}^{\text{RLPD}}$ , which were subsequently used to further SFT  $\pi_0$ , yielding  $+\mathcal{D}^{\text{PLD}}$ ,  $+\mathcal{D}^{\text{Human}}$ , and  $+\mathcal{D}^{\text{RLPD}}$ .

**Performance and failure modes.** Across 30 randomized trials per task, all methods achieved perfect success on peg insertion (30/30), demonstrating robust reactive skills. In cube pick-up, however,  $+\mathcal{D}^{\text{RLPD}}$  and  $+\mathcal{D}^{\text{Human}}$  succeeded in only 16/30 and 10/30 trials, respectively, while  $+\mathcal{D}^{\text{PLD}}$  maintained 30/30. Figure 7 illustrates a typical failure: policies trained on  $\mathcal{D}^{\text{RLPD}}$  or  $\mathcal{D}^{\text{Human}}$  often pushed the cube into the upper-left corner, where the gripper became stuck. By contrast,  $+\mathcal{D}^{\text{PLD}}$  was reliably recovered by repositioning the cube before grasping. Distribution analysis confirms that neither human demonstrations nor RL rollouts visited such corner states, whereas **PLD** explicitly probed the base policy and generated diverse trajectories that captured these cases. This explains its robustness and highlights its potential as a self-improving data flywheel.<sup>1</sup>

**Robustness for long-horizon tasks.** To evaluate the robustness of **PLD** in executing long-horizon and dexterous manipulation tasks, we set up two 6-DoF YAM robot arms developed by *I2RT-Robotics* (2025). We consider an industrial insertion task—specifically, inserting a micro graphics card into a motherboard. To enable fully autonomous operation without human intervention or re-setting, we decompose the task into four stages: Stage 1: Pick up the GPU from the table and insert it into slot 1. Stage 2: Move the GPU from slot 1 to slot 3. Stage 3: Firmly insert the GPU into slot 3. Stage 4: Unplug the GPU from slot 3 and place it back on the table. A reward classifier is trained to govern the state machine that coordinates these stages. After at most 8 hours of training for each subtask and distilling the learned skills into a generalist VLA policy (implementation described in Section G.4), the system can continuously perform the full task loop without human assistance for at least 1 hour. As shown in the video, although the one-shot success rate for each stage is not 100%, the system is capable of recovering from failures, keeping the data flywheel running autonomously.

## H.1 GENERALIZATION PERFORMANCE

We perform SFT of  $\pi_0$  on *Pick Up Blue Cube (Clean Env)* and *Peg Insertion* data, and evaluate the fine-tuned policy on *Pick Up Blue Cube (Cluttered Env)* and *Pick Up Red Cube (Cluttered Env)* tasks. The results in Table 6 show that VLA SFT on **PLD** data achieves better generalization performance compared to human teleoperation data.

Table 6: Comparison of PLD vs Human Data on real-world tasks (success rate).

SR Dataset	PLD Data	Human Data
Pick Up Blue cube (cluttered Env)	28/30 (93.3%)	12/30 (40.0%)
Pick Up Red cube (cluttered Env)	20/30 (66.7%)	10/30 (33.3%)
Peg Insertion	30/30 (100.0%)	30/30 (100.0%)

<sup>1</sup>Generalization results are reported in Section H.

1350  
1351  
1352  
1353  
1354  
1355  
1356  
1357  
1358  
1359  
1360  
1361  
1362  
1363  
1364  
1365  
1366  
1367  
1368  
1369  
1370  
1371  
1372  
1373  
1374  
1375  
1376  
1377  
1378  
1379  
1380  
1381  
1382  
1383  
1384  
1385  
1386  
1387  
1388  
1389  
1390  
1391  
1392  
1393  
1394  
1395  
1396  
1397  
1398  
1399  
1400  
1401  
1402  
1403

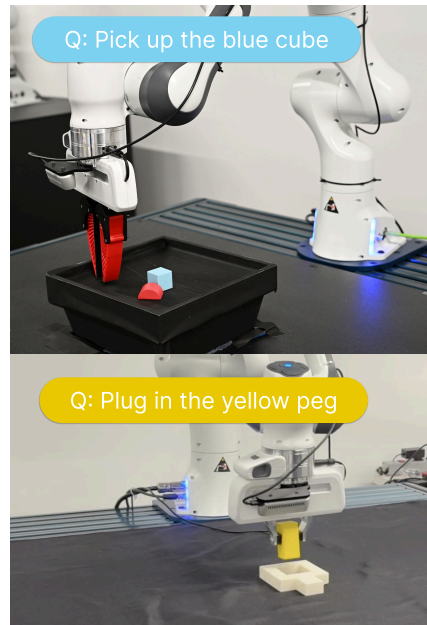


Figure 19: Franka Panda real-world setup for manipulation tasks.

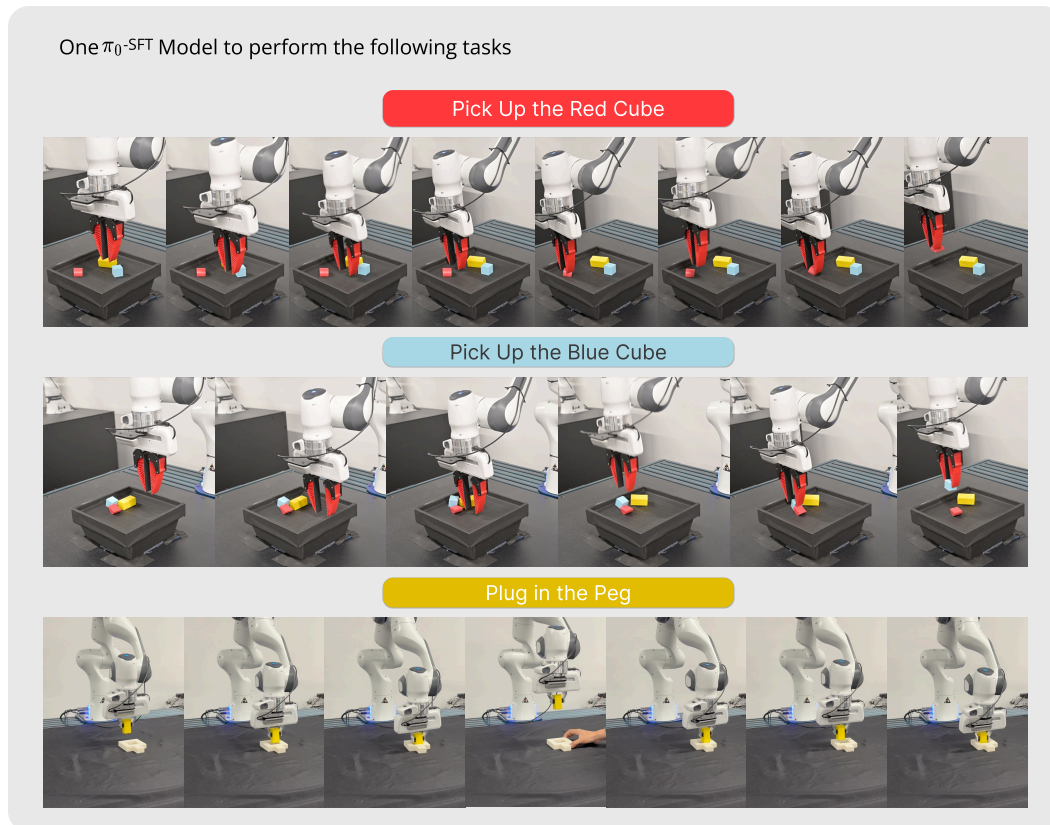


Figure 20: **Real-world Generalization Performance.** We evaluate one model’s multi-task performance on three language-conditioned manipulation tasks including pick-and-place and peg insertion.